Dy^{3+} DOPED $KCa(PO_3)_3$ PHOSPHOR FOR WHITE LIGHT GENERATION: STRUCTURAL AND LUMINESCENT STUDIES

Thesis Submitted in
Fulfillment of the Requirement for the
Award of the Degree of

MASTER OF SCIENCE
in
Physics

Submitted By

SANDIP MAURYA	**(2K22/MSCPHY/34)**
DEEPTI	**(2K22/MSCPHY/58)**

Under the supervision of
Prof. A.S. RAO

Department of Applied Physics
Delhi Technological University

To the
Department of Applied Physics

DELHI TECHNOLOGICAL UNIVERSITY
(Formerly Delhi College of Engineering)
Shahbad Daulatpur, Main Bawana Road, Delhi – 110042
June, 2024

DEPARTMENT OF APPLIED PHYSICS

DELHI TECHNOLOGICAL UNIVERSITY

(Formerly Delhi College of Engineering)

Bawana road, Delhi – 110042

ACKNOWLEDGEMENTS

Firstly, and importantly, we would like to thank our supervisor **Prof.A.S.Rao** (Department of Applied Physics) for allowing and giving us the golden opportunity to work in Materials And Atmospheric Science Research Laboratory without his mentoring and unconditional support, this work would not have been possible. We would like to thank him for his valuable time, feedback and suggestions. We sincerely thank him for his patience in correcting manuscripts and hope to carry forward the various nuances we learned during the writing process. His approach to scientific inquiry kept the joy of research alive during this research. Further, we would like to thank all the lab staff to provide us healthy environment. The success of work depends upon the nature of the working environment. We also extend our thanks to all the faculty members, M.Sc.(Physics) scholars and members of the Department of Applied Physics, Delhi Technological University for their suggestions and valued support. Lastly, we would also like to thank our parents for their enduring support and for believing in us always.

Place: Delhi

Date: 07/06/2024

SANDIP MAURYA

DEEPTI

DECLARATION

We hereby certify that the work which is presented in the Major Project-II entitled **"Dy^{3+} doped $KCa(PO_3)_3$ phosphor for white light generation: Structural and Luminescent Studies"** in fulfilment of the requirement for the award of the Degree of Master of Science in Physics and submitted to Department of Applied Physics, Delhi Technological University, Delhi is an authentic record of our own, carried out during a period from 2023-2024, under the supervision of **Prof. A.S. Rao**, Department of Applied Physics, Delhi Technological University, Delhi.

The matter presented in this thesis has not been submitted by us for the award of any other degree of this or any other Institute/University. The work has been published/accepted/communicated in SCI/SCI expanded/SSCI/Scopus indexed journal OR peer reviewed Scopus indexed conference with the following details:
Title of the paper: **Dy^{3+} doped $KCa(PO_3)_3$ phosphor for white light generation: structural and luminescent studies.**
Author names: Deepti, Sandip Maurya, and A.S. Rao
Name of Journal: Physica Scripta, Institute Of Physics (IOP) Publication.
Status of paper (Accepted/Published/Communicated): Published
Published Date of paper communication: February 29, 2024
Date of paper acceptance: May 20, 2024
Date of paper publication: May 30, 2024
Have you registered for the conference? : Yes
Name of Conference: International Conference on Atomic, Molecular, Material, Nano, and Optical Physics with Application (ICAMNOP).
Conference Dates with venue: December 20-22, 2023, Delhi Technological University

Sandip Maurya	Deepti
Roll No.: 2K22/MSCPHY/34	Roll No.: 2K22/MSCPHY/58

SUPERVISOR CERTIFICATE

To the best of my knowledge, the above work has not been submitted in part or full for any Degree of Diploma to this University or elsewhere. I further certify that the publication and indexing information given by the students is correct.

Place: Delhi

Date: 07/06/2024

Prof. A.S.Rao
(DEPARTMENT OF APPLIED PHYSICS, DTU)

SUPERVISOR

DEPARTMENT OF APPLIED PHYSICS
DELHI TECHNOLOGICAL UNIVERSITY
(Formerly Delhi College of Engineering)

Bawana road, Delhi – 110042

CERTIFICATE

I, hereby certify that the Project Report titled " **Dy^{3+} doped $KCa(PO_3)_3$ phosphor for white light generation: Structural and Luminescent Studies** " Which is submitted by **SANDIP MAURYA, Roll No 2K22/MSCPHY/34, and DEEPTI , Roll No 2K22/MSCPHY/58** from Department of Applied Physics, Delhi Technological University, Delhi in fulfilment of the requirement for the award of the degree of Master of Science, is a record of the project work carried out by the students under my supervision. To the best of my knowledge this work has not been submitted in part or full for any Degree or Diploma to the university or elsewhere.

Place: Delhi
Date: 07/06/2024

A Rao

SUPERVISOR

Prof. A.S. Rao
Department of Applied Physics
Delhi Technological University

Abstract

Using the traditional solid-state reaction approach, Dy^{3+} ions doped $KCa(PO_3)_3$ phosphors have been synthesized to investigate their luminescent properties to produce high-quality white light for solid-state lighting applications, particularly in white LEDs. X-ray diffraction (XRD) patterns were used to examine the structure and phase of the phosphors. Using scanning electron microscopy (SEM), the morphology of the as-synthesized phosphor has been investigated. Fourier transform infrared spectroscopy (FT-IR) has been used to investigate several vibrational bands seen in the phosphor. Using diffuse reflectance spectra (DRS), the as-synthesized phosphors' optical band gap values have been estimated. When Dy^{3+} ions are excited at 350 nm, the photoluminescence (PL) spectra characteristics observed for the activated $KCa(PO_3)_3$ phosphor show strong white area emission due to both 575 nm, which is related to the $^4F_{9/2} \rightarrow {}^6H_{13/2}$ and 482 nm that is ascribed to $^4F_{9/2} \rightarrow {}^6H_{15/2}$ transition of Dy^{3+} ions. Additionally, the concentration quenching of Dy^{3+} ions doped at 4 mol% is seen in the PL spectra. Based on the observed PL spectra, the computed CIE chromaticity coordinates for the optimised $KCa(PO_3)_3$ phosphors are located in the deep white area. The lifespan of the astitled phosphors decreases as the amount of Dy^{3+} ions increases in the host lattice. Additionally, the PL decay profiles shows a dual exponential behaviour when excited at 350 nm, with an emission wavelength at 575 nm. The lifetime values were used to calculate the quantum efficiency of the as prepared phosphors. On the basis of the results of the aforementioned studies, we wish to project Dy^{3+} ion doped $KCa(PO_3)_3$ phosphors as white light generating materials in w-LEDs and for other photonic applications.

CONTENTS

LIST OF TABLE

LIST OF FIGURE

LIST OF ABBREVIATIONS

LED	**Light Emitting Diode**
WLED	**White Light Emitting Diode**
RE	**Rare Earth**
XRD	**X-Ray Diffraction**
PL	**Photoluminescence**
JCPDS	**Joint Committee on Powdered Diffraction Standards**

CHAPTER 1: INTRODUCTION

1. Phosphor:

Phosphors are materials that exhibit the phenomena of photoluminescence when excited by electromagnetic radiation. These are solid inorganic material host lattices that have been intentionally doped with an activator to enhance the absorption of electromagnetic radiation. A number of different types of phosphors with varied host lattices and activators or dopants have been synthesized each having its own characteristic emission color and emission time, the time the phosphor glows for after the radiation event[1]. This makes phosphors suitable for a variety of applications ranging from lighting solutions, laser devices, display devices, and energy applications to temperature sensors.

Fig 1:- Phosphor materials

Photoluminescence in a phosphor occurs when the electrons of the phosphor are excited to higher energy level upon absorption of photons. These excited electrons may lose their energy via radiative or non- radiative mechanisms to return to their ground state and during this relaxation process, they emit photons whose energy lies in the visible range and appear to us as light of various color as shown in Fig.1. This time is usually in the range of 10^{-8} s after which they come back to ground state by losing the extra energy in the form of a photon. The time period between absorption and emission varies greatly and may range from milli-seconds to even days. This absorption and emission is primarily done by the activator electrons and mostly rare-earth ions are used as activators for the host lattice due to their superior luminescent properties

1.1 Phosphor Synthesis

Phosphors can be synthesized using:

1. **Solid-state reaction method,**
2. Sol-gel synthesis,
3. Hydrothermal,
4. Co-precipitation methods, etc. effectively.

The precursors in the form of oxides, nitrates, sulphides are taken to form the phosphor material. The size as well as shape of the phosphor particle can be controlled and tuned by the selection of the synthesis technique and hence depending upon the required application a suitable synthesis technique must be used to get a phosphor with desirable properties.

CHAPTER 2: THEORETICAL FRAME WORK

2. Luminescence of materials:

Materials that emit light in addition to black body emission are known as luminescent materials. an incident energy source into electromagnetic wave output in the ultraviolet (UV), visible, or infrared regions of the spectra[2]. Luminescence can be classified on the basis of the simulation that is provided and the Table 2 given below summarizes it.

Table 2: Types of luminescence and their origin

DESIGNATION	**STIMULATED BY**	**TRIGGER**	**ACRONYM**
PHOTOLUMINESCENCE	UV, Visible Photons	Light	PL
RADIOLUMINESCENCE	X-Ray, Gamma ray, Charged Particle	-	RL
CATHODOLUMINESCENCE	Energetic Electron	-	CL
ELECTROLUMINESCENCE	Collisional excitation of internal electron accelerated	Applied Electric Field	EL
THERMOLUMINESCENCE	Photons, Charged Particles	Heat	TSL

2.1.1 Difference between fluorescence, phosphorescence and chemiluminescence:

- Photoluminescence is classified into fluorescence and phosphorescence.If the substance’s glow is triggered by light, then it is photoluminescence, whereas if the glow is caused by a chemical reaction, then it is chemiluminescence.

Fluorescence and phosphorescence are both caused by a substance's capacity to absorb the light and subsequently release the light with a longer wavelength and consequently less energy.

- The basic difference between these two phenomena is the time taken to complete the
- Process. In the case of fluorescence, the emission occurs immediately, so it can be observed only when the light source is kept on (for example, UV lights); however, in the case of phosphorescence, the absorbed light energy can be stored for a period of time and then released later, as a result, even after the light source has been switched off, there is an afterglow.
- To conclude, if it fades away quickly, it is fluorescence; if it lasts longer, it is phosphorescence. It's chemiluminescence if it requires some type of activation.
- A good example of it can be considered if we imagine a scenario at the nightclub: Teeth Materials that emit light in addition to black body emission are known as luminescent materials**,** eyes and fabric glowing under the black light are considered fluorescent, the emergency exit sign is phosphorescent and the glow sticks are chemiluminescent.

2.2 Rare earth (RE) materials:

- There are 17 rare earth (RE) elements in periodic table. Scandium, Yttrium and some 15 other lanthanide series elements come under this category.
- Since, all RE elements are metals, therefore they are sometimes known as the "Rare Earth metals".
- Rare earth elements are commonly employed as catalysts, phosphors, and polishing agents. In air pollution management, illuminated screens in electronic devices, and a variety of other applications rare earth elements are commonly used[1].

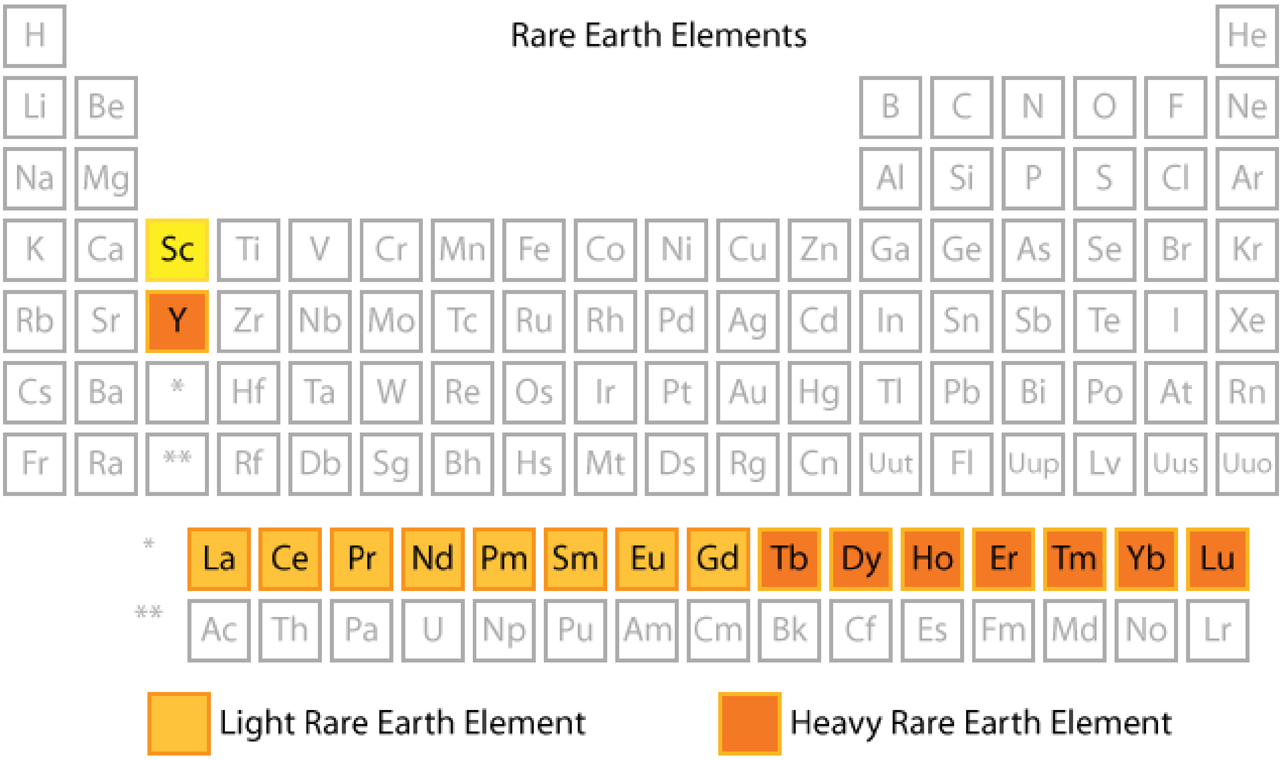

Fig 2:- Location of Rare Earth elements in the periodic table

- Actually, rare earth elements are not "rare" as the name suggests. For example, the two least abundant rare earth elements are Thulium and Lutetium but each of them has an average crustal abundance approximately 200 times more than that of the gold. Although these metals are not rare but are quite tough to mine as it is uncommon to obtain these metals in enough concentrations for economical extraction.

- Yttrium, cerium, lanthanum and neodymium come under the category of the most abundant rare earth elements. The average crustal abundances for these elements are similar to some of the most frequently used industrial metals for instance chromium (Cr), nickel (Ni), zinc (Zn), and lead (Pb) etc. But again, they can rarely be found in extractable concentrations.

2.2.1 Ions of rare earths acting as co- and activator-activators:

Dopant or activator ion" refers to a luminous centre integrated into a host matrix. Dopant- containing inorganic solids fall under the standard group. These ions function as a centre of luminosity and are in charge of the pertinent electronic transitions in phosphor. Certain metals can also function as "sensitizers" or co-activators in host materials, absorbing excitation energy and transferring it to the activators in the process. In spite of this, using RE.

2.2.2 Lattice hosts for phosphors triggered by RE

When making rare earth-activated phosphors, selecting the perfect lattice is essential. Low lattice phonon energy and strong radiative transitions are desirable characteristics for host lattices. High chemical stability, a regulated emission profile, and high emission efficiency are also requirements for host materials. The environment around activator ions has a significant impact on their luminescence.

2.3 White LEDs:

The manufacture of White LEDs (Light Emitting Diodes) at the lowest possible cost has been a major area of study in recent years. Several materials that emit diverse colours have been found to be doped with rare earth elements, including silicates, borates, and aluminates. Maintaining the right balance of the current blue, yellow, green, and red emitting phosphor to recover the resulting white color emission is a difficult challenge. More dopants are needed to prepare white LEDs with two or three phosphors, which raises the price of the LEDs or display devices. At least two prominent emission bands are present in the yellow region (470–500 nm) of rare earth-dysprosium ions because of the $^4F_{9/2}$ to $^6H_{15/2}$ transition, and in the blue region (560–600 nm) because of the $^4F_{9/2}$ to $^6H_{13/2}$ transition. It is feasible to white[3] light.

Why Dy3+ Doped Phosphors Are Selected for White Light Emission.

For white light emission, several studies have employed Dy3+ as a single dopant in several hosts. The explanation for this can be summed up as follows:

- Low price
- Thermally and chemically stable

Low Cost:

To create a white light generating source, we require blue, green, and red emitting phosphors in the right amounts. We need at least two distinct phosphor matrices doped with various rare earth elements in order to achieve the same result, which could be expensive. When only a few Dy3+ doped phosphors are used, only one dopant and one host are needed to provide white light emission, significantly lowering the cost.

Stable Both Chemically and Thermally:

The majority of silicate and aluminate phosphors are highly resistant to chemical and heat degradation. Neither rising temperatures nor any chemicals have an effect on their composition. This is among the justifications for using these silicate and aluminate phosphors as a material for the emission of white light.

CHAPTER 3: EXPERIMENTAL TECHNIQUE:

3.1 Materials & Methods:

The most common methods to prepare a phosphor are solid state method, hydrothermal, co-precipitation and sol-gel method. Out of these four techniques, solid state method has been the most popular and quite feasible so far in the research field. The key feature of this (SSM) is that it is widely applicable to prepare all kinds of compositions of phosphor like oxide or non-oxide systems. We have all kinds of options available as dopants and co-dopants to give a variety to our phosphor system which becomes quite easy using this technique. There are minor chances of the sample being prone to some kind of impurities but that can be avoided using the crucibles made of noble metals like Gold, Platinum, etc.

3.1.1 *Solid State Approach*

In order to create a new solid with a well-defined structure, solid-state synthesis, also known as the ceramic method, is frequently utilized to initiate a chemical reaction from solid starting components. by calcinations at a high temperature to permit the cations to diffuse among themselves after milling the suitable metal oxides or carbonates[4].

This process is frequently used to create monovalent cations, transition metal phosphates, and arsenates in single crystals and polycrystalline powder.

3.1.2 *Sample Preparation: $KCa(PO_3)_3: Dy^{3+}$*

We have selected KCa(PO3)3 as the Host matrix and synthesised it by Solid State Reaction Method.

$K_2CO_3+CaCO_3+NH_4H_2PO_4$

Mixed and grinded for 1hrs. in Agate Mortar and Pestle

Heating in furnace at 600˚C for 5 hrs

Sample Prepared

Grinded for further Characterizations

Fig 3.1.2:- Furnace used for sintering

3.2 Characterization Techniques:

3.2.1 XRD

The bending of light around an obstacle's corners is referred to as diffraction. It is a prerequisite for the occurrence of diffraction. The obstacle's size must be almost equal to the light frequency being employed. Like other electromagnetic radiation, X-rays can also be diffracted; however, in order to do so, the obstacle's size must be a few angstroms (about 1 Å), which is also the frequency of X-rays. This is because the atomic gap in the crystal is nearly a few Å. The constructive interference of monochromatic x-rays is the basic principle of XRD. X-rays are directed towards the sample under investigation, and sample's crystal structure causes the X-rays to spread in a variety of directions. It is recorded by a detector and further amplified to be analysed on a monitor screen.

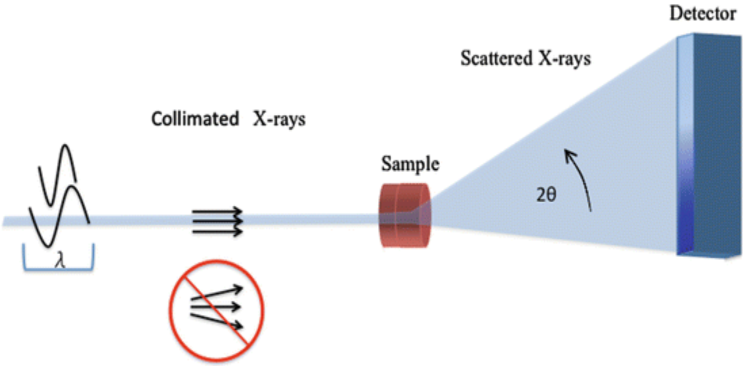

Fig 3.2.1(a):- A demonstration of x-rays being scattered by the sample

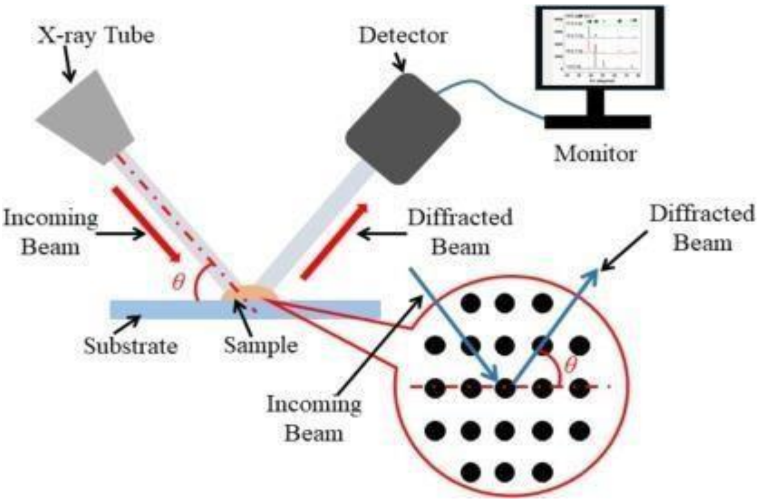

Fig 3.2.1(b):- Experimental setup for XRD analysis

Bragg's Law:

According to this law, an x-ray will reflect at the same angle of scattering (θ) if it is encountered upon a crystal surface at an angle of incidence (θ). An interference pattern is visible if the path difference (d) is a whole number (n) multiple of the wavelength (λ).

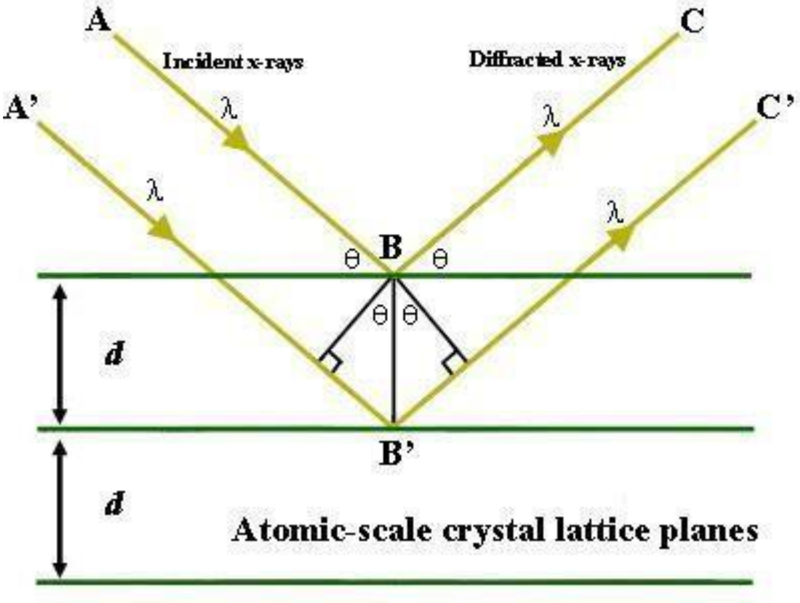

Fig 3.2.1(c):- Diagram showing the incident and diffracted x-rays from the crystal surface.

Bragg's Law is:

$$n\lambda = 2d\sin(\theta)$$

Here, d is the distance between the crystal layers (i.e., path difference), θ is the angle of incidence, and n is the diffraction order. λ is the x-ray incident wavelength.

Method of X-Ray Diffraction (XRD):

1. Laue's Photographic Method
2. Bragg's X-Ray Spectrometer Method
3. Rotating Crystal Method
4. **Powder Crystal Method**

Since we have used powder method, so elaborating on that:

The sample to be tested is homogenized and ground into a fine powder. The powdered sample is then struck on a hair and mounted vertically in the axis of a cylindrical camera with a piece of gum. A monochromatic beam is permitted to fall on it, various possibilities exist. A few particles may emerge from the random alignment of tiny crystals. For each set, there is the probability of reflections in different orders. In addition, another proportion of grains will have a different set of planes in the appropriate positions for reflections to occur.

3.2.2. Photoluminescence (PL) Spectroscopy:

Photoexcitation (PL) spectroscopy is a kind of light-emitting spectroscopy in which light emission results from a mechanism known as photoexcitation[5]. The electrons within the material travel to the 18 energized locations (excitation) as the light is directed towards the sample. Once energy has been released in non-radioactive forms, the electron goes down to an intermediate level called the conduction band. Thereafter, when electrons flow from the conduction band to their ground states, energy can be released in the form of light (called radiative relaxation). This phenomenon is shown in fig. 9. The experimental setup is quite similar to that of Absorption spectroscopy except for the monochromators near the source. PL spectroscopy is beneficial to estimate the electronic structure and assets of the compound as it provides the peak light intensity that objects can emit at a certain wavelength.

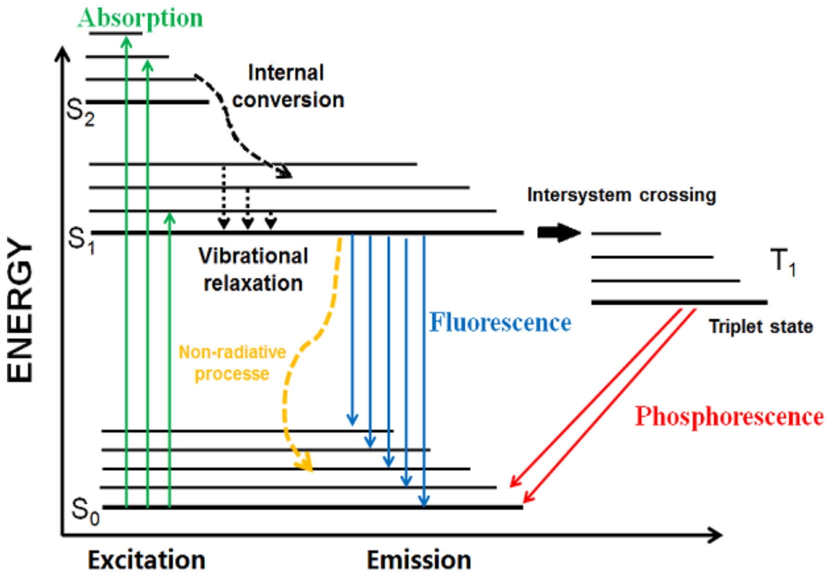

Fig 3.2.2:- Phenomenon of Photoluminescence

3.2.3. **Scanning Electron Microscope (SEM)**

This is a type of electron microscope that produces images of a sample by scanning it with a focused beam electrons. The electrons interact with atoms in the sample, producing various signals that can be detected and translated into an image.

This is a multivariate statistical analysis technique that is used to analyze structural relationships. This technique combines factor analysis and multiple regression analysis, and it is used to analyze the structural relationship between measured variables and latent constructs.

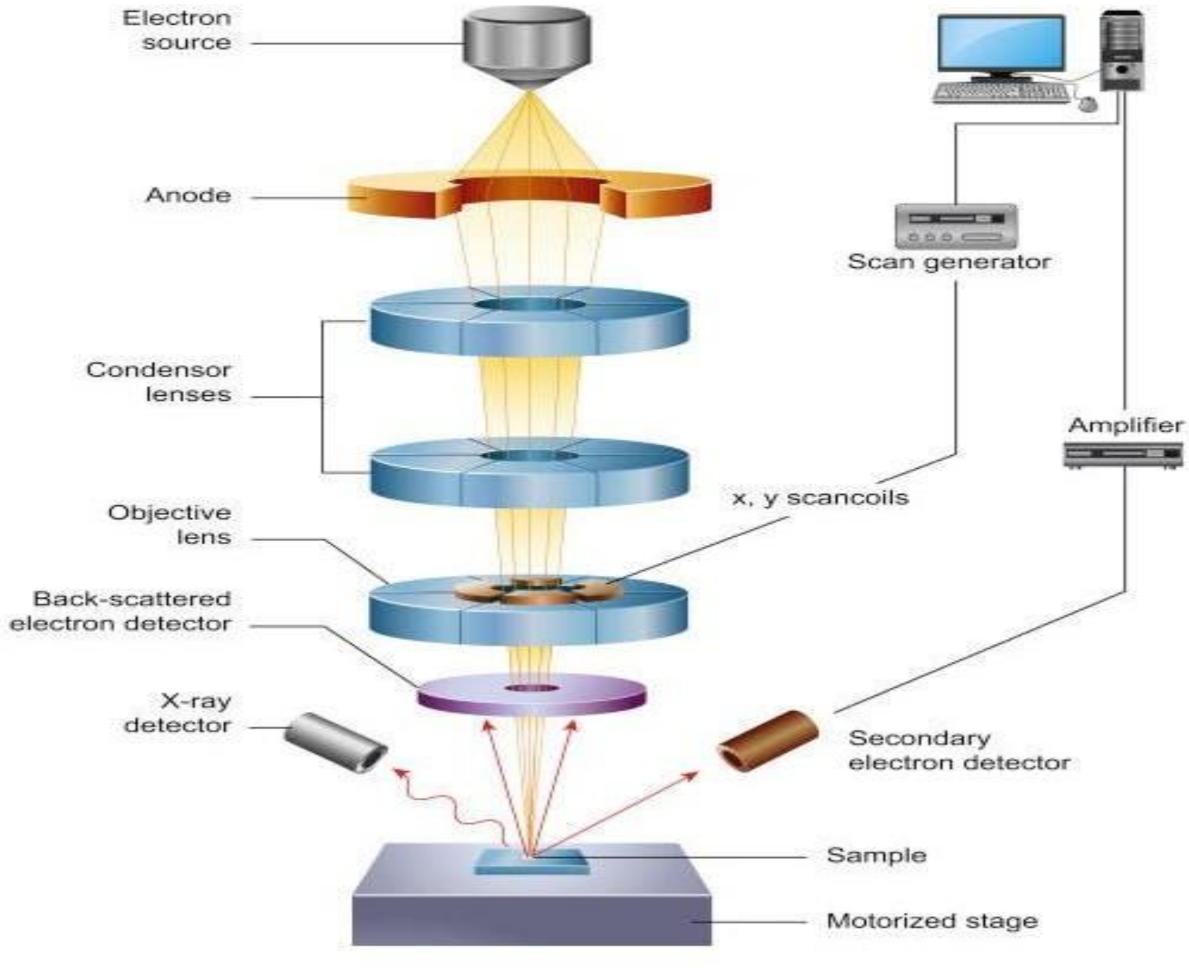

Fig 3.2.3:- Schematic diagram of scanning electron microscope

3.2.4. Fourier Transform Infrared Spectroscopy (FT-IR):-

Fourier Transform Infrared Spectroscopy (FTIR) is an analytical technique used to identify organic, polymeric, and, in some cases, inorganic materials. It provides information about the molecular composition and structure of samples by measuring their infrared spectra.

Infrared light is passed through a material by the FT-IR device, with some of it being absorbed but some traveling through. Resulting output at the detector is a spectrum that ranges from 4000 cm-1 to 400 cm-1 and indicates the chemical fingerprint of the material. FT-IR analysis is a good approach for chemical identification since every molecule has its unique spectral fingerprint. The various bands are marked in the transmittance versus wavenumber plot. These bands correspond to the different modes of stretching namely, the symmetric, asymmetric, bending, and so on

Fig 3.2.4:- Schematic diagram of FT-IR

3.2.5. Diffuse Reflectance Spectroscopy (DRS):-

This is a technique used in the analysis of solid samples, particularly powders. It measures the diffuse reflectance of a sample, which is useful in fields like materials science, geology, and chemistry for characterizing the optical properties and composition of materials.

Diffuse reflectance spectroscopy is a very well-established approach for examining the spectral features of impenetrable solid materials, based on the principle that certain light reflected from the substance is reflected inwardly and also from the surface.

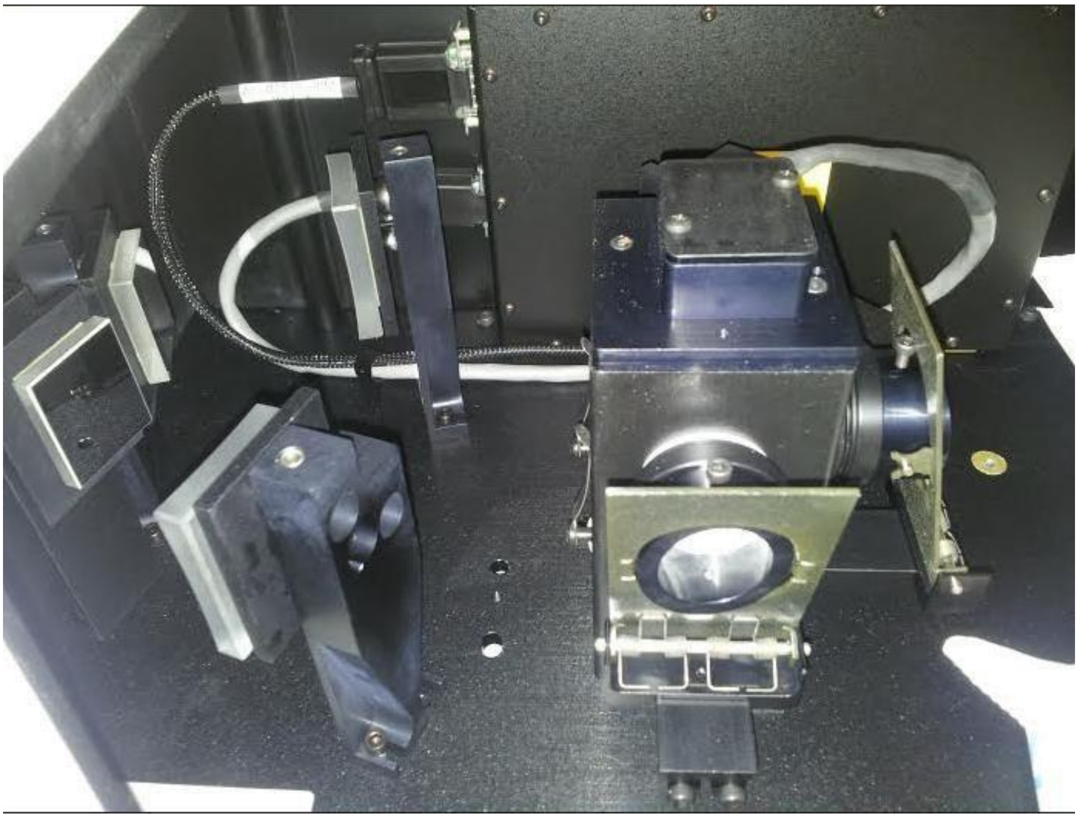

Fig 3.2.5:- Schematic diagram of DRS

CHAPTER 4: Dy^{3+} Doped $KCa(PO_3)_3$ phosphor for white light generation: Structural and Luminescent Studies

Introduction

Phosphors are widely used in solid-state lighting, display devices, and anti-counterfeiting applications. White light-emitting diodes (w- LEDs) have gained popularity in recent years due to their low power consumption and environmental benefits. They are expected to replace traditional light sources such as tungsten halogen lamps and incandescent lamps. LEDshave a significantly longer lifespan when compared to other lighting technologies like Low- Pressure Sodium (LPS) and fluorescent lights. The longevity of LEDs far surpasses that of incandescent lights. The latest LED lights can last for over 50,000 to 100,000 hours or more. In contrast, incandescent bulbs have a lifespan that is only 1-5% as long at best, lasting for approximately 1,200 hours The additional features of these properties include a broad spectrumof colors that span from ultraviolet to infrared, a limited spectral bandwidth, a high degree of luminous efficiency, and an extremely rapid response time. The most common method forcreating white LEDs is to combine phosphors with UV or n-UV chips made of InGaN. The development process of the standard LED involves three crucial steps: seasoning, selection, and certification. These steps are meticulously carried out to ensure the optimal performance of the w-LED[6]. During seasoning, the LED is subjected to a series of tests to stabilize its electrical and thermal properties. The selection process involves choosing the most suitablew-LED based on its characteristics and performance[7]. Finally, the certified LED undergoes rigorous testing to ensure its compliance with industry standards and specifications. Generally,phosphors consist of an activator, a host material, and sometimes a sensitizer. Rare earth or metals are often used as activator ions for doping. Red, green, blue, and white light can be produced by doping one or more rare earth (RE) ions in an appropriate single matrix. Selectinga suitable substrate material is crucial for obtaining energy-efficient phosphors.

Phosphates are crucial luminescent materials that offer various crystal-field environments for emission centers. Phosphates doped with rare-earth-elements (REEs) are thermally stable and have a rigid tetrahedral matrix that is ideal for charge stabilization. Moreover, they are excellent host materials for producing phosphors as they require low sintering temperatures. Researchers have recently explored alkali and alkaline-earth-metal phosphate phosphors to develop new materials for UV-based w-LEDs[8]. Many studies have focused on $AB(PO_3)_3$ phosphates, with A representing monovalent cations (Li^+, Na^+, K^+, and Cs^+) and B representingdivalent cations (Ca^{2+}, Sr^{2+}, and Ba^{2+})[9]. These phosphates have efficient thermal and hydrolytic stabilities, making them ideal host materials for w-LEDs.

$KCa(PO_3)_3$ has a unique structure comprising of twisted polyphosphate rings forming a cyclic anion $(P_{12}O_{36})^{12-}$, where non-bridging oxygen atoms point toward the center[9–12]. This structure creates a distorted octahedral coordination environment for the central potassium ions and distorted octahedral cavities for calcium ions between the rings. $KCa(PO_3)_3$ possesses desirable properties such as low phonon energy, high optical damage threshold, good charge stabilization, and chemical stability, making it a suitable host material for lanthanide activators. Additionally, $KCa(PO_3)_3$ exhibits transparency in the spectra range of interest and low sintering temperature. Ca-based phosphate compounds are of interest to researchers due to their significant UV absorption and serving as an important host for luminescence.

Dysprosium (Dy^{3+}) doped luminescence materials have been gaining increasing attention for their superior white emissions[13–15]. When incorporated in various host matrices, Dy^{3+} ion is known to display two prominent emission bands in its spectra. The first band corresponds to the pseudo-quadrupole transition $^4F_{9/2} \rightarrow {}^6H_{13/2}$, which involves a change in both ($\Delta L=2$) and ($\Delta J=2$). This transition occurs at a wavelength of 576 nm and is characterized by a yellow emission color, while the second band is associated with the transition $^4F_{9/2} \rightarrow {}^6H_{15/2}$ at 478 nm (blue). One can achieve almost white emission using Dy^{3+} doped luminescent materialsby manipulating the yellow-bluish intensity ratio (Y/B)[13]. Therefore, Dy^{3+-} -activated phosphors have emerged as a promising option for developing white light. Researchers have foundthat Dy^{3+}-activated phosphors offer advantages over other options in terms of their ability to produce white light. Therefore, they are considered a strong candidate for use in a variety of applications.

In our work, we have synthesized a series of polyphosphates, or $KCa(PO_3)_3$, (KCP) doped with Dy^{3+} phosphor. This study examines the structural and luminescent properties of KCP: Dy^{3+} phosphors, emphasizing the analysis of the concentration quenching mechanism, luminescence decay characteristics, and color perception. The ultimate goal of this study was to achieve white light emission through the utilization of the prepared phosphors. The results of this examination hold great potential for making significant advancements in the field of materials science.

4.1 Experiment section

4.1.1. *Sample Preparation*

A series of Dy^{3+} doped phosphors $KCa(PO_3)_3$ at different concentrations of Dy^{3+} ions (i.e. 1.0, 2.0, 3.0, 4.0, and 5.0 mol%) was prepared via solid-state reaction technique usingK_2CO_3(99%, Fisher Scientific), $CaCO_3$(98.0-100.5%, Fisher Scientific), $NH_4H_2PO_4$(99%,Fisher Scientific), and Dy_2O_3(99.98%, Thermo Scientific) as raw materials. After mixing the raw materials in a stoichiometric ratio with acetone for 1 h in an agate mortar, the powder wasthen transferred into the alumina crucible. The resulting powder was heat-treated at 673 K for3 h in the furnace to eliminate carbonates. And then, the powder was sintered at 873 K for 5 hours in an air atmosphere. Finally, the powder was ground again in an agate mortar into a finepowder for further characterization.

4.1.1 *Experimental Techniques*

Using the Bruker Model D8 Advance equipment, which was built to produce nickel-filtered Cu-Kα radiation (0.154nm), the XRD spectra of the prepared materials was observed in the 2θ range of 20º to 80º. Using a JEOL 7610 F Plus SEM machine, surface morphology was recorded. An un-doped phosphor's FT-IR spectrum was captured with a Perkin-Elmer Frontier FT-IR spectrometer, ranging from 400 to 4000 cm^{-1}. DRS was obtained for the Dy^{3+}-doped phosphors in the 200–1400nm wavelength range using a JASCO model V-923 UV–Vis–NIR spectrophotometer. A JASCO FP-8300 spectrofluorometer with a resolution of 0.1 nm was used to capture the PL excitation and emission spectra for each Dy^{3+}-ion doped phosphor under a Xenon excitation source. Luminescent decay curves were measured using an Edinburgh FL920 Fluorescence Spectrometer. Each measurement was carried out at room temperature.

4.2 Results and Discussion

4.2.1 X-Ray Diffraction (XRD) Analysis

The crystallographic arrangement and phase purity of the un-doped $KCa(PO_3)_3$ phosphors were examined using XRD patterns. The hexagonal crystal structure $KCa(PO_3)_3$ (JCPDS No. 39-1408) is a member of the P-6c2 (188) space group. Every diffraction peak is precisely matched to the JCPDS 39-1408 standard card's peaks as shown in Fig 4.2.1. With the lattice coordinates a=6.8077 Ǻ, b=6.8077 Ǻ, and c=10.3730 Ǻ as well as α=90°, β=90°, and γ=120°, it suggests the samples are in single-phase[9,11]. The XRD patterns of the phosphor $KCa(PO_3)_3$ that were in linewith the previously described JCPDS database showed that the phosphor had successfully synthesized with a high level of purity. The addition of Dy^{3+} ions, demonstrates that the synthesized phosphors are devoid of any contaminating phases. One K site and one Ca site were present in the $KCa(PO_3)_3$ host and they both shared the six-fold coordination. Due to the similarity in their ionic radii Ca^{2+}(radii = 1.00 Å) and Dy^{3+}(radii = 0.908 Å), the Dy^{3+} ions chose to occupy the Ca^{2+} site when incorporated into the host, $KCa(PO_3)_3$. The as- titled phosphors exhibit strong and distinct diffraction peaks, indicating their high crystallinity—a prerequisite for comparatively superior luminosity.

.

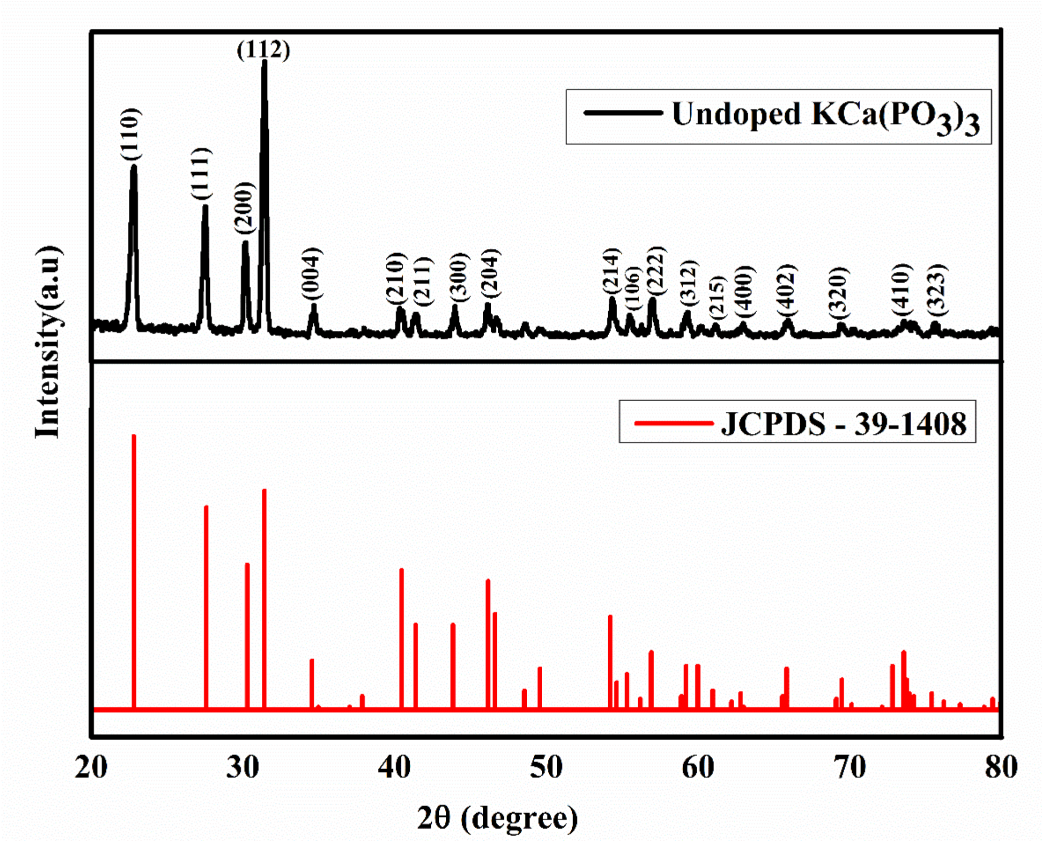

Fig 4.2.1:- XRD pattern of un-doped $KCa(PO_3)_3$ phosphor along with standard diffraction pattern (JCPDS) 39-1408.

4.2.2 Morphological Analysis from SEM

The morphology and particle size information of the prepared phosphors is better understood by examining FE-SEM pictures of an undoped and 4.0mol% doped $KCa(PO_3)_3$ phosphor.

$KCa(PO_3)_3$ powder phosphors have an uneven polyhedron shape and unequal particle size, as shown in Fig 4.2.2 (a,b). The high-temperature reaction method and manual grinding have also resulted in very low agglomeration of some phosphor particles. Most of the phosphor particles available in the market today are between 2 and 10 µm in size[16]. The ImageJ Software is used tofind the size of the particle for an un-doped and 4.0mol% of Dy^{3+} ions doped $KCa(PO_3)_3$ phosphor. The sizes fall in the region of 3-5 µm. As a result of the samples' particle sizes being in the micrometer range, these materials can be aptly used for coating white LEDs anddisplay devices[13]. Furthermore, energy dispersive X-ray analysis (EDX) has been used to analyze the elemental makeup of the as-synthesized phosphors. The EDX for the doped $KCa(PO_3)_3$: 4 mol% Dy^{3+} phosphor is presented in Fig 4.2.2(c). Every precursor element is visible inthe phosphor lattice, according to the EDX picture.

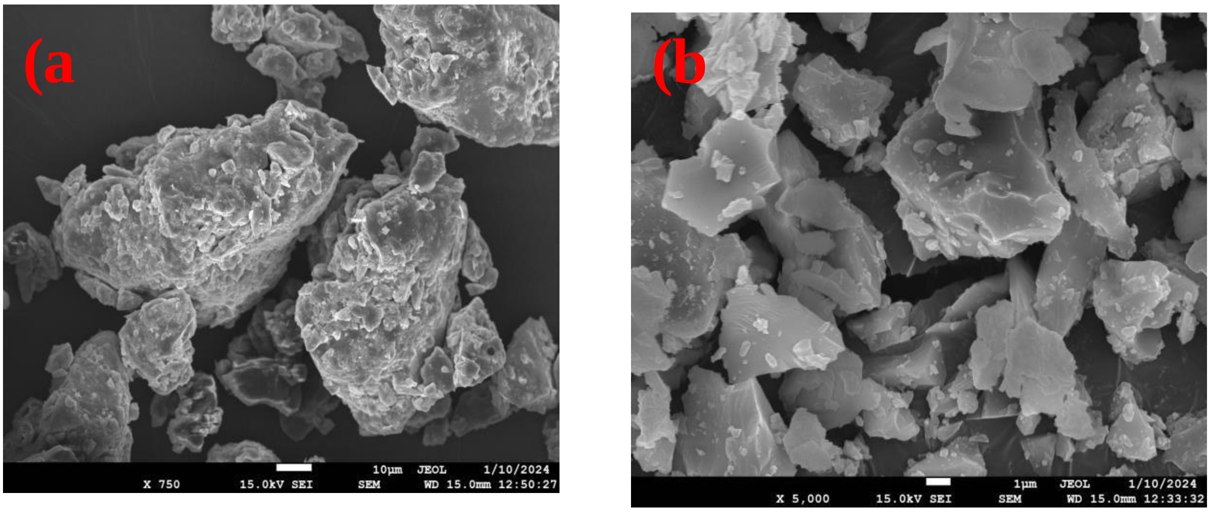

Fig 4.2.2:- SEM image recorded For (a) an un-doped (b) 4.0 mol% of Dy^{3+} ion doped $KCa(PO_3)_3$

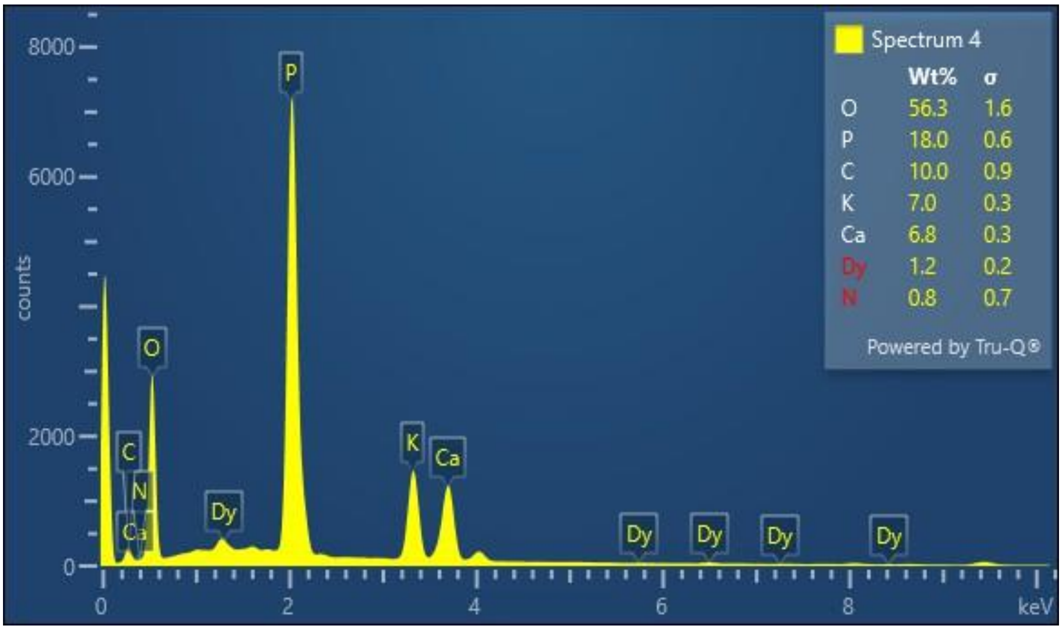

Fig 4.2.2(c):- EDX image of $KCa(PO_3)_3$: xDy^{3+} (x= 4 mol%) phosphor .

4.2.3 FT-IR Analysis

Vibrational spectroscopy (FT-IR) was conducted to investigate the bonding properties of un-doped $KCa(PO_3)_3$ phosphor[17]. The vibrational spectrum of the prepared phosphor shown in Fig 4.2.3 was recorded from 400 cm^{-1} to 4000 cm^{-1}, which exhibited multi-vibrational bands. The spectrum showed bands at 493, 764, 1038, 1105, 1251, 1394, 2901, 2989, 3675, and 3749 cm^{-1}.The stretching vibrations of the PO_2 were recorded in the 1000–1200 cm^{-1} and 1200–1400 cm^{-1} ranges, for the symmetric and asymmetric stretching, respectively, while the bending vibrations were detected in the range of 400–550 cm^{-1}. The vibrations of the P-O-P oxygen bridges were detected in the region of asymmetric mode (1000–1050 cm^{-1}) and symmetric mode (600–800 cm^{-1}).

The measured FT-IR spectra matched well with the theoretical considerations presented earlier. The observed bending vibrational wavenumbers correspond to specific normal modes, with the asymmetric stretching (O-P-O) showing a strong vibration at 1251 cm^{-1} and the symmetric stretching (O-P-O) exhibiting a very strong vibration at 1105 cm^{-1}. Similarly, the asymmetric stretching (P-O-P) showed a very strong vibration at 1038 cm^{-1}, and the symmetric stretching (P-O-P) had a strong vibration at 764 cm^{-1}. The antisymmetric stretching of bonded water molecules and the presence of hydroxyl radicals were indicated by the peaks observed at 2901

cm^{-1} and 2989 cm^{-1}, respectively. The band observed at 3675 cm^{-1} was responsible for the stretching peak of the hydroxyl group. The multi-component patterns of these spectra showed the same number of bands as those reported in previous works for ABP3O9-type compounds.

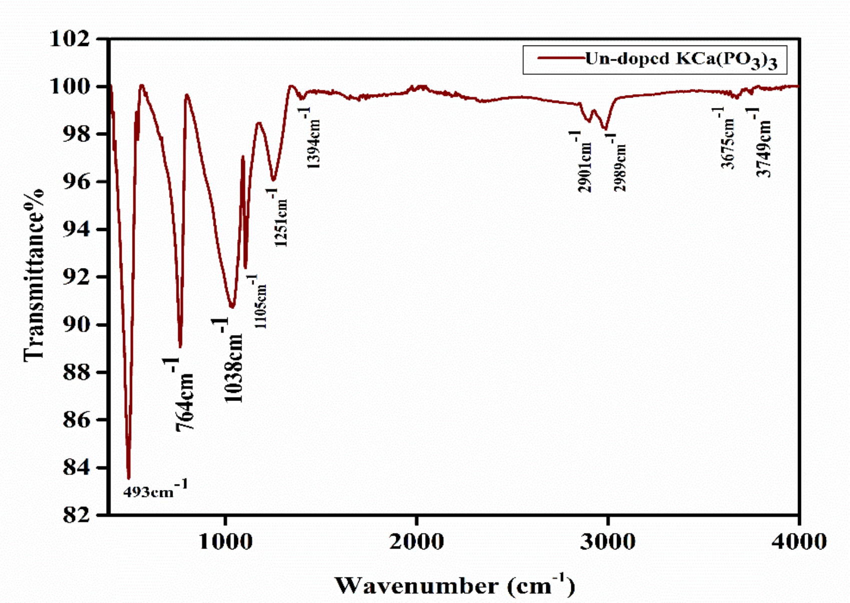

Fig 4.2.3:- FT-IR Spectrum of un-doped $KCa(PO_3)_3$ phosphor.

4.2.4 Diffuse Reflectance Spectra (DRS) Analysis

Phosphors utilized in w-LEDs have an optical band gap (E_g), a crucial parameter. The DRS of undoped and KCP:xDy^{3+}, x = 4 mol% is shown in Fig 4.2.4(a). Between 200 and 1400 nm. The DRS spectral data were converted into the Kubelka-Munk function, and the optical band gap was then calculated using the following equation.

$$F(R) = \frac{1-R^2}{2R} = \frac{\alpha}{s} \qquad (1)$$

Here, R stands for sample reflectance, S for scattering coefficient, and α for absorption coefficient[18]. The equation shows the following relationship between energy bandgap (E_g) and absorption coefficient (α).

$$\alpha h\nu = (h\nu - E_g) \qquad (2)$$

Here, n can have values of 2 or 1/2, corresponding to indirect and direct transitions, respectively, depending on the kind of transition. C is an energy-independent constant (in the current case, = 1). The unit of photon energy is $h\nu$. Since α is exactly proportional to F(R), the above equation can be expressed in this way:

$$F(R)h\nu = C(h\nu - E_g)^n \qquad (3)$$

To determine the band gap for the KCP:Dy^{3+} phosphor, a tauc plot was created b/w hν and $[F(R)h\nu]^{1/2}$. The optical band gap (E_g) can be derived by extrapolating the linear portion of the plot[19]. The plot is shown in Fig 4.2.4(b) and the calculated E_g values for undoped and optimisedKCP phosphors are 4.60 and 4.49 eV respectively.

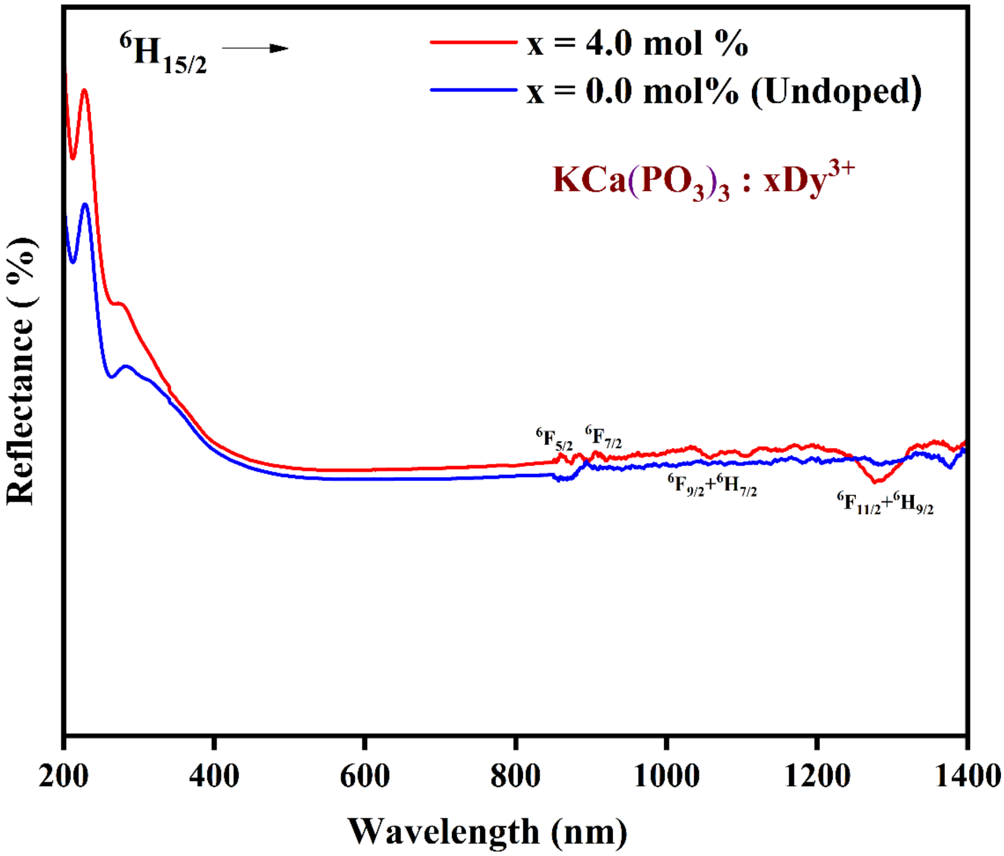

Fig 4.2.4(a):- Diffuse reflectance spectra of undoped and $KCa(PO_3)_3$: xDy^{3+} (x= 4 mol%)phosphor.

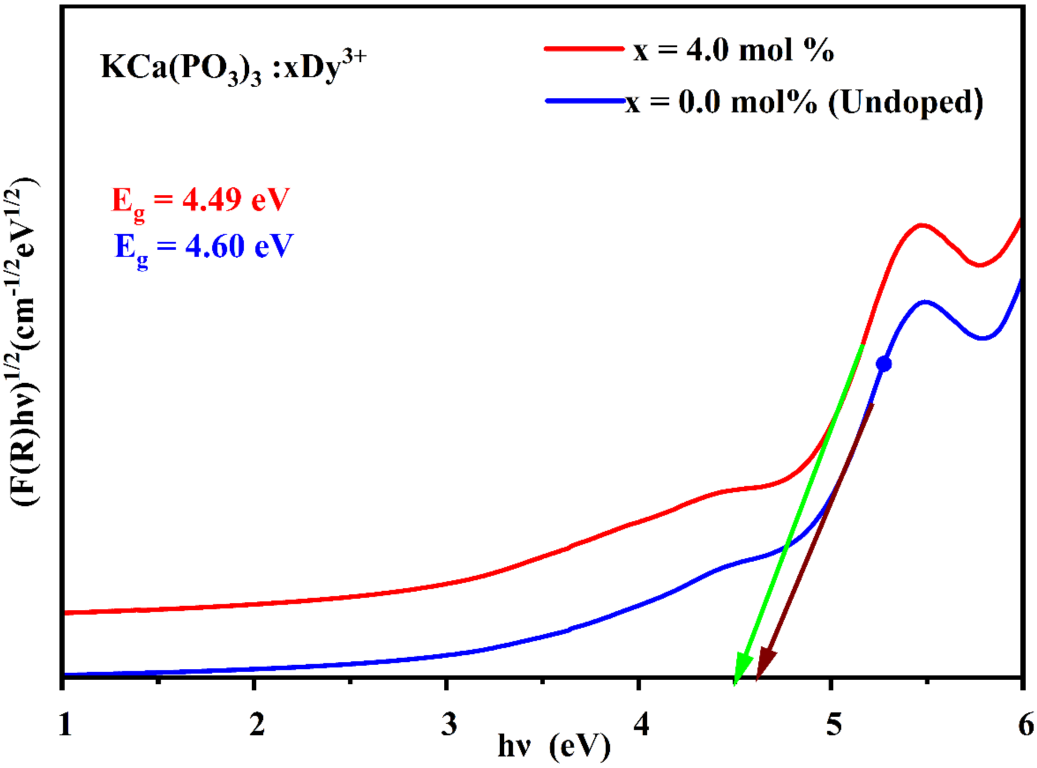

Fig 4.2.4(b):- Tauc plot for direct optical band gap of undoped and $KCa(PO_3)_3$: xDy^{3+} (x= 4 mol%)phosphor.

4.2.5. Photoluminescence Spectral Analysis (PL) of $KCa(PO_3)_3$

4.2.5.1 *Excitation Spectra*

The excitation spectra of KCP: xDy^{3+} (x=1, 2, 3, 4, 5 mol%) phosphors is shown in Fig. 4.2.5.1(a). Several sharp excitation peaks have been detected within a specific range of wavelengths (290-500 nm)[20]. There are 5 primary peaks of the excitation spectra that are caused by the f-f electronictransitions of Dy^{3+}ions, with the maximum excitation wavelength situated at 350 nm. The electronic transitions responsible for these peaks are $^6H_{15/2}$ to $^4M_{17/2}$ [298 nm], ($^6P_{3/2}$) [324nm], $^6P_{7/2}$ [350nm], $^6P_{5/2}$[364nm], ($^4I_{13/2}$ + $^4F_{7/2}$) [386nm], and $^4I_{15/2}$[453nm]. The KCP: Dy^{3+}

Phosphor is suitable for excitation by near-UV LEDs, as indicated by the main excitation bands at 350-400 nm.

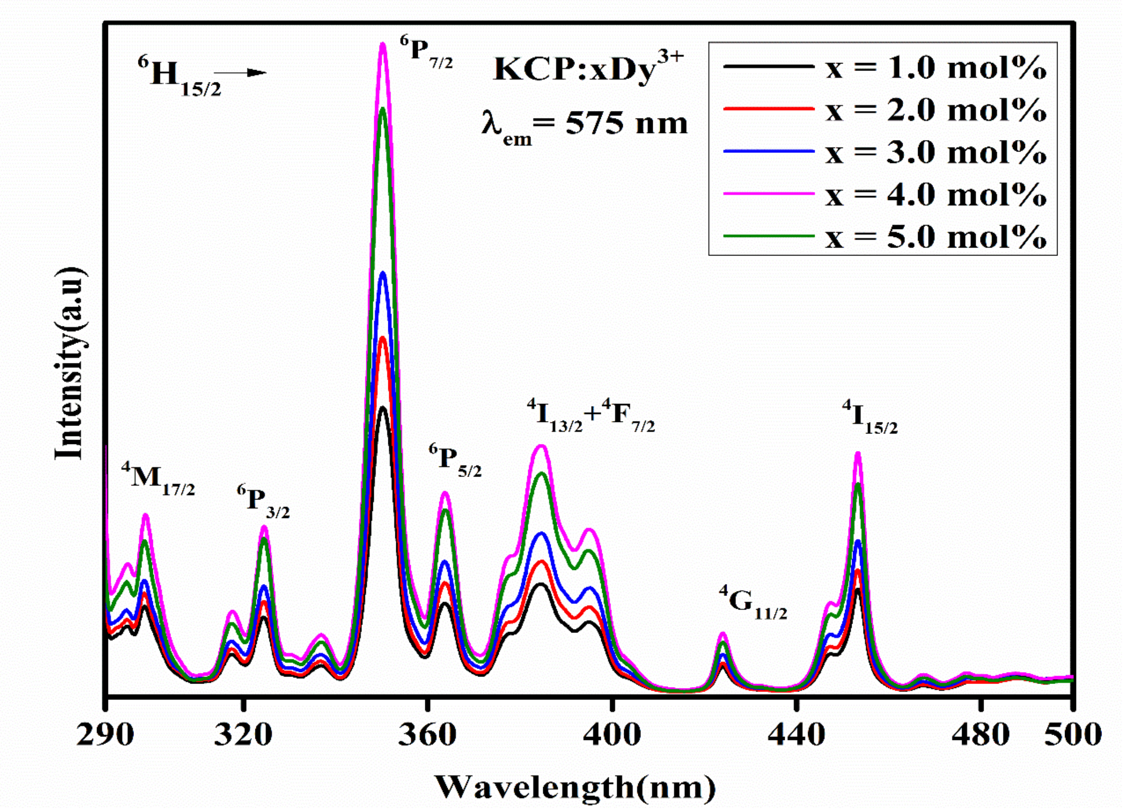

Fig 4.2.5.1(a):- Excitation spectra of Dy^{3+} ions doped KCa(PO3)3 phosphors under 575 nm emissionwavelength.

4.2.5.2 ***Emission Spectra***

The emission spectra of KCP: xDy^{3+} (x=1, 2, 3, 4, 5 mol%) shown in Fig 4.2.5.2(a) were examined under 350 nm excitation. We found that the emission shape and position didn't change significantly with the increase in the concentration of Dy^{3+} doping, except for the emission intensity[21]. The spectra showed two strong characteristic peaks; at 482 nm corresponding to blueemission and 575 nm corresponding to yellow emission, which were attributed to the transitionfrom $^4F_{9/2}$ to $^6H_{15/2}$ and $^6H_{13/2}$, respectively and weak peaks observed at 665 nm (red emission)ascribed the transition $^4F_{9/2}$ to $^6H_{11/2}$. Our observations suggest that the optical characteristics of KCP: Dy^{3+} are directly impacted by the configuration of the host material in which they areembedded. When the Dy^{3+} ion is positioned at a site with high symmetry, i.e. a site that has aninversion center, the yellow emission is the predominant outcome. However, when the Dy^{3+} ion is positioned at a position without a center of symmetry, which is typically a site exhibitinglow symmetry, its emission intensity is observed to be considerably amplified[12]. The emission of yellow light with a wavelength of 575nm ($^4F_{9/2}$-$^6H_{13/2}$) is a result of a forced dipoletransition (electric transition). This type of transition happens only at low symmetries withoutan inversion center. The intensity of this emission is highly dependent on the crystal-field environment. We found that its intensity increases immensely as a function of Dy^{3+} concentration. The blue band's intensity corresponding to the 482nm ($^4F_{9/2} \rightarrow ^6H_{15/2}$) dipole transition, (which refers to the change in the magnetic moment during a transition between energy levels), is known to exhibit a relatively low sensitivity to the effects of crystal fields. The analysis of emission spectra suggests that the concentration of Dy^{3+} has a significant impact on the intensity of the blue transition $^4F_{9/2} \rightarrow ^6H_{15/2}$. Specifically, an increase in Dy^{3+} concentration up to 4% results in increased emission intensity. But beyond this concentration, there is a discernible drop in emission intensity. The strength of the $^4I_{13/2} \rightarrow ^6H_{15/2}$, $^4I_{15/2} \rightarrow ^6H_{15/2}$, and $^4F_{9/2} \rightarrow ^6H_{11/2}$ transitions, however, rapidly dropped as the concentration of Dy^{3+} increased. The observed evolution is a result of the concentration quenching phenomenon and the impact of population on the $^4I_{15/2}$ and $^4I_{13/2}$ energy levels[22]. The amplified resonant energy transfer from the excited energy state to the low energy or ground state ($^4F_{9/2} \rightarrow ^6H_{15/2}$) of the nearby Dy^{3+} ion, as well as the cross-relaxation phenomenon between theexcited Dy^{3+} ion (donor) and the ground Dy^{3+} ion (acceptor), are responsible for the increase in quenching intensities with increasing Dy^{3+} ion concentration.

At 4 mol% concentration of Dy^{3+}, concentration quenching occurred. However, when the concentration of these ions becomes too high, the possibility of energy transfer between ions rises. As a result, more excitation energy is transferred via non-radiative processes, resulting in decreased luminescence efficacy. To examine the energy transmission mechanism between Dy^{3+} ions, we computed the critical distance[16]. The Blasse theory equation may be used to determine the critical radius distance R_C.

The Blasse equation is:

$$R_c \approx 2\,[\frac{3V}{4\pi X_c N}]^{\frac{1}{3}} \qquad (4)$$

Where N is the number of cations per unit cell (N = 2), X_C is the threshold concentration of Dy^{3+} (X_C = 0.04), and V is the volume per unit cell (V = 416.33*10^4 Å).

The critical distance (R_c) between activator and sensitizer ions in $KCa(PO_3)_3{:}xDy^{3+}$ was 21.50 Å, indicating that non-radiative energy transfer predominantly occurs through exchange contacts or multilayer interactions. For energy transfer to occur, the activator and sensitizer need to be positioned close to each other within the lattice. Additionally, there should be significant overlap in their wave functions, which allows for electron exchange to take place. The critical distance for this exchange is less than 5 Å, but the calculated R_C values were much higher, indicating that energy transfer between Dy^{3+}-Dy^{3+} ions in $KCa(PO_3)_3{:}xDy^{3+}$ happens through multilevel interactions.

According to the Dexter theoretical model:

$$\log\left(\frac{I}{x}\right) = A - \frac{s\log(x)}{d} \quad (5)$$

Where A signifies a constant, d represents the mixture's dimensions (= 3) and I is the emission intensity. We use the value of s to identify the type of multilevel interactions. The typesof interactions, including closest neighbor ion, dipole-dipole, dipole-quadrupole, and quadrupole-quadrupole interactions, are quantified by their respective multipole moments[16]. Specifically, these interactions are represented by the values of 3, 6, 8, and 10 for the corresponding multipole moments respectively. To study the values of s, we select samples with x=0.01, 0.02, 0.03, 0.04, and 0.05. Subsequently, we determine the emission intensity and generate a linear graph of KCP:xDy^{3+} that is shown in Fig.4.2.5.2(b) between log(I/x) vs log(x). The (s/3) value is determined by analyzing the gradient of the linear plot b/w log(I/x)and log(x). Upon analyzing the data, we found that the slope is -1.40712. This value helped usdetermine that the value of s is 4.2214, which is less than 6. This suggests that energy transferdue to nearest neighboring ions is the primary mechanism causing concentration quenching in the sample. Asymmetric molecules exhibit inherent dipoles because of the unequal distribution of electronsaround the positively charged nucleus[23]. The dipole-dipole interaction's dimension is determinedby the two dipoles' center distance and relative orientation. The interaction is computed using the potential energy of each dipole. Concentration quenching results from a substantial energy exchange between activators that happens when the concentration of activators reaches a certain level. The schematic energy level diagram shown in Figure 4.2.5.2(c) illustrates the possible electronic transitions of the Dy^{3+} in the $KCa(PO_3)_3$ polyphosphate phosphor. Thehigher energy level ($^6P_{7/2}$) of the Dy^{3+} ions becomes populated by Dy^{3+} excitation (350 nm). Due to inadequate energy difference between the states to produce a radiative transition, the ions undergo non-radiative transitions (phonon relaxation) from the excited level to the groundstate ($^4F_{9/2}$)[24]. Ultimately descends to the various ground-level states ($^6H_{15/2}$, $^6H_{13/2}$, and $^6H_{11/2}$) to release blue, yellow, and red photons, which are associated with the Dy^{3+} ion transitions at $^4F_{9/2} \rightarrow {}^6H_{15/2}$, $^4F_{9/2} \rightarrow {}^6H_{13/2}$, and $^4F_{9/2} \rightarrow {}^6H_{11/2}$.

This energy exchange reduces the amount of luminous energy levels and lessens the intensity of the fluorescence. The three cross-relaxation processes of Dy^{3+} are as follows[8]:

CRC 1: ($^4F_{9/2}$+ $^6H_{15/2}$ → ($^6H_{9/2}$, $^6F_{11/2}$) + $^6F_{3/2}$)

An initial Dy^{3+} ion descends from level $^4F_{9/2}$ to the intermediate level ($^6H_{9/2}$, $^6F_{11/2}$), while another Dy^{3+} ion is excited from the ground state level $^6H_{15/2}$ to level $^6F_{3/2}$.

CRC 2: ($^4F_{9/2}$+ $^6H_{15/2}$ → ($^6H_{7/2}$, $^6F_{9/2}$) + $^6F_{5/2}$)

An initial Dy^{3+} ion descends from level $^4F_{9/2}$ to the intermediate level $^6H_{7/2}$+$^6F_{9/2}$, while another Dy^{3+} ion is excitedfrom the ground state level $^6H_{15/2}$ to level $^6F_{5/2}$.

CRC 3: ($^4F_{9/2}$+ $^6H_{15/2}$ → $^6F_{1/2}$ + ($^6H_{9/2}$, $^6F_{11/2}$))

An initial Dy^{3+} ion descends from level $^4F_{9/2}$ to the intermediate level $^6F_{1/2}$, while another Dy^{3+} ion is excited from the ground state level $^6H_{15/2}$ to level $^6H_{9/2}$+$^6F_{11/2}$[25].

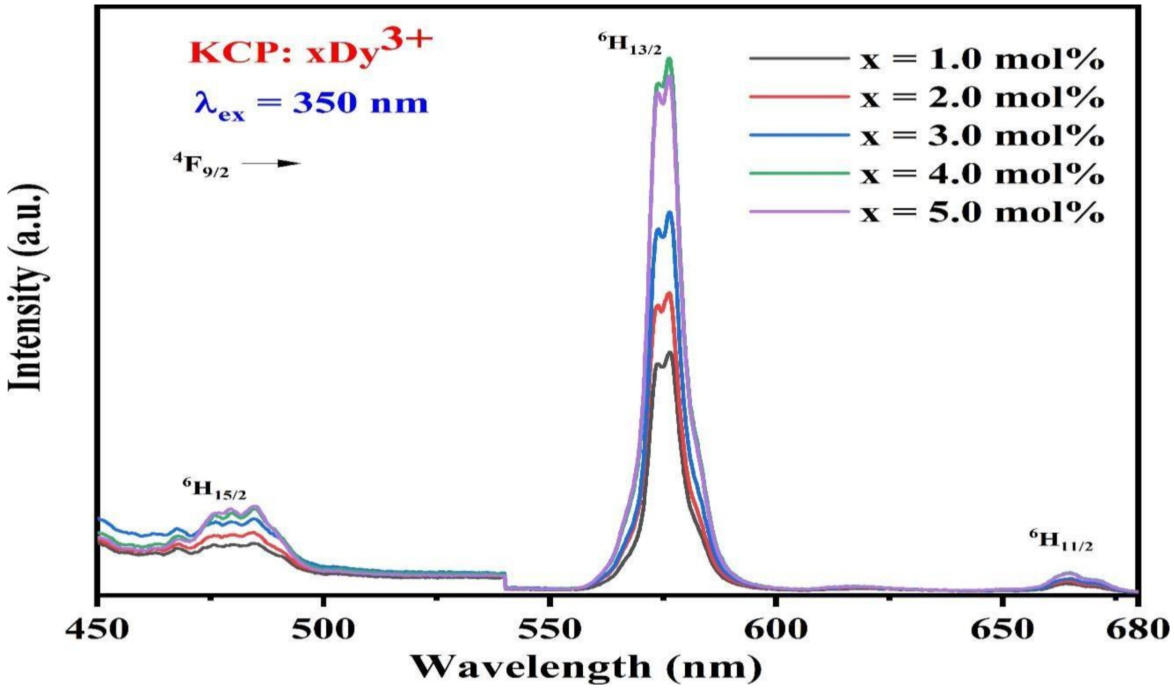

Fig 4.2.5.2(a):- Emission spectra of Dy^{3+} ions doped $KCa(PO_3)_3$ phosphors under 350 nm excitation wavelength.

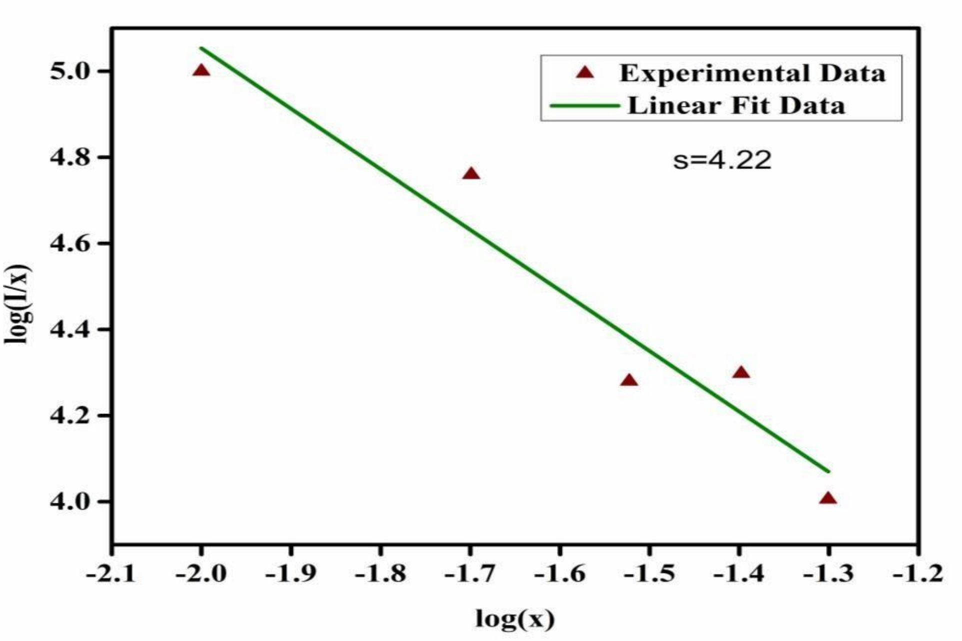

Fig4.2.5.2(b):- Plot of log (I/x) with log(x).

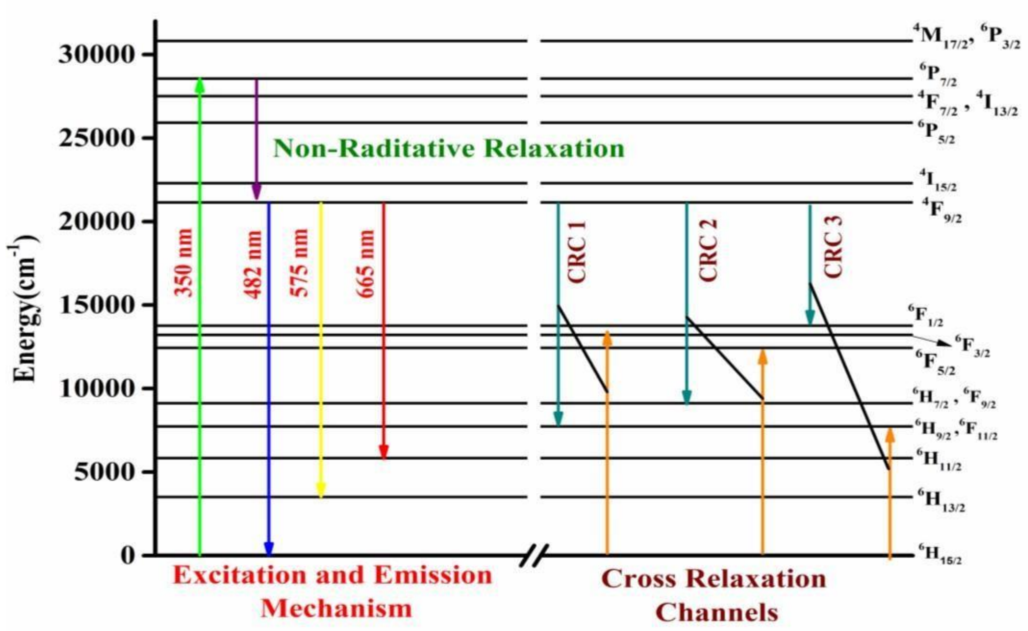

Fig4.2.5.2(c):- Partial energy level diagram and possible cross-relaxation channels of Dy^{3+} ion doped $KCa(PO_3)_3$ phosphor.

4.2.5.2.1 Y/B RATIO

The luminescence intensity and the site symmetry of RE ions are generally inversely related. Solid-state lighting appliances prioritize the Dy^{3+} ion because it emits the main colors that are necessary for the creation of white light. In general, white light can be produced by precisely balancing blue and yellow light. As seen in Fig 4.2.5.2(a), the yellow band's intensity (at 575 nm) is comparatively higher than the blue band's intensity (at 350 nm). The production of white light is significantly influenced by the intensity ratios of the blue and yellow bands, which are the ratios of their combined intensities. The concentration of dopant (in this case, Dy^{3+}) ions, the host phosphor matrix, and the excitation source all have an impact on the yellow-to- blue (Y/B) intensity ratio[26]. The Y/B intensity ratio is significantly impacted by the inversion symmetry and local coordination surrounding nearby Dy^{3+} ions. Moreover, it is found that the local coordinated regions around Dy^{3+} ions are the least symmetric with respect to neighboring atoms in the absence of inversion symmetry. Due to the increased covalency, the emission spectrum exhibits an intense yellow band as opposed to a blue one. Y/B intensity ratios are comparatively more than 1, indicating that light is being generated in the white area. The higher Y/B ratios support the high covalent nature of Dy^{3+} ions. Consequently, the KCP:Dy^{3+} 4.0 mol in the as-prepared KCP phosphors shows the highest Y/B value and, consequently, the maximum covalency[27].

4.2.6 CIE Co-ordinate

To understand the colorimetric performance of $KCa(PO_3)_3$: xDy^{3+} ions (x = 1.0, 2.0, 3.0, 4.0, 5.0 mol %) phosphor, the "Commission Internationale de I'Eclairage" (CIE) chromaticity coordinates at λ_{ex} = 350 nm were acquired from the emission spectrum data. The Fig.4.2.5.6(a) displays the calculated CIE coordinates for every as-synthesized $KCa(PO_3)_3$ phosphor at λ_{ex} = 350 nm and λ_{em} = 576 nm. The coordinates of the as-synthesized Dy^{3+} doped $KCa(PO_3)_3$ phosphors, as indicated in the CIE diagram lie near the central white region. This indicates that $KCa(PO_3)_3$ phosphors doped with Dy^{3+} ions are suitable for solid-state lighting and plasma display panels[28]. Another important component in colorimetric computations used to look into color saturation is color purity (CP). The estimation of CP can be done using formula below:-

$$cp = \sqrt{\frac{\sqrt{(x-x_{\underline{i}})^2+(y-y_{\underline{i}})^2}}{(x_d-x_i)^2+(y_d+y_i)^2}}$$

where (x, y) represents the color coordinates of the $KCa(PO_3)_3$ phosphor, (x_{ee}, y_{ee}) stands for equal energy point, and (x_d, y_d) indicates points of dominant wavelength. The Dy^{3+} (x = 4.0 mol%) ions doped $KCa(PO_3)_3$ phosphor is found to have 16% color purity under 350 nm excitation. When triggered by blue or n-UV light, Dy^{3+} (x = 4.0 mol%) ions doped $KCa(PO_3)_3$ phosphor can be used as a white emitting component in w-LEDs.

When determining whether a light source is warm or cold, one of the most crucial parameters is the correlated color temperature (CCT). CCT is determined using the equation below.

$$CCT = -449n^3 + 525n^2 + 6823.3n + 5520.32 \quad (7)$$

The color coordinates are n=(x-0.332)/(0.1858-y). The prepared phosphor is a cool emission source, as indicated by the assessed CCT values as mentioned in Table 4.2.6. The calculated CCTvalues of the KCP:xDy^{3+} phosphors are significantly more than 4000 K, indicating that cool white light can be created from these phosphors[29].

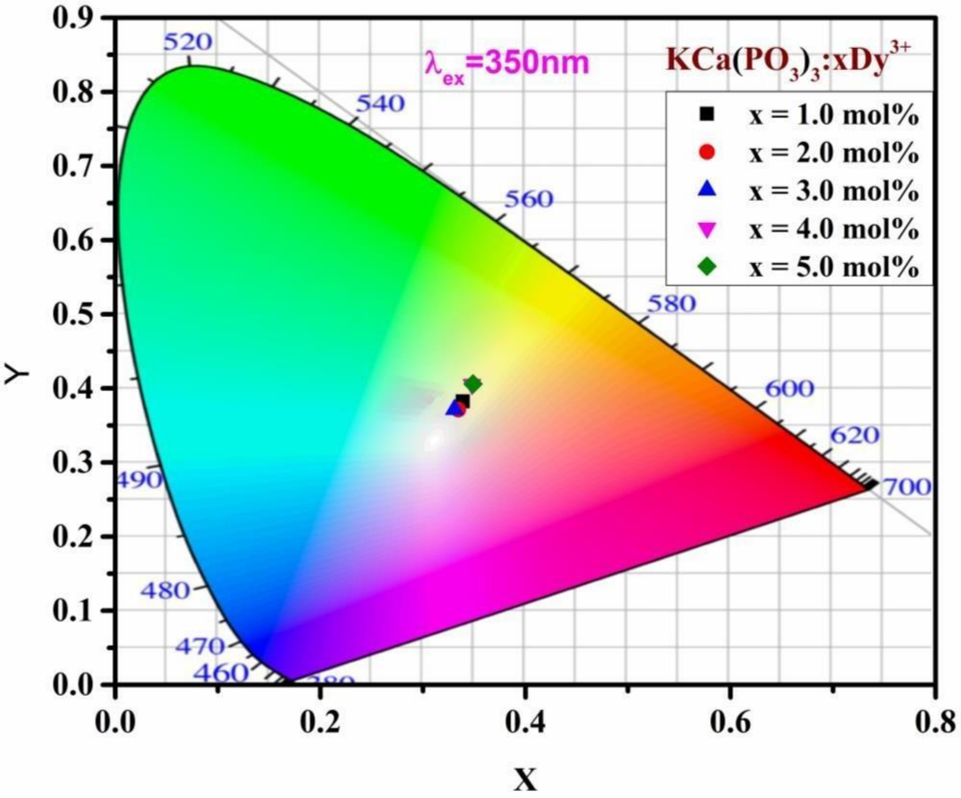

Fig 4.2.6:- CIE chromaticity coordinates of Dy^{3+} ions in $KCa(PO3)3$ phosphors.

Table 4.2.6: CIE coordinates, CCT values of KCP: xDy^{3+} (x=1.0, 2.0, 3.0, 4.0, 5.0 mol%) under350 nm excitation wavelength.

Sample ID KCP: xDy^{3+}	**CIE coordinates** **(x, y)**	**CCT values** **(K)**
x = 1.0mol%	(0.338, 0.382)	5287.127
x = 2.0mol%	(0.334, 0.371)	5428.813
x = 3.0mol%	(0.330, 0.371)	5570.698
x = 4.0mol%	(0.367, 0.405)	4497.287
x = 5.0mol%	(0.368, 0.405)	5056.40

4.2.7 Photoluminescence (PL) Decay

The PL decay patterns under room temperature λ_{ex} = 350 nm and λ_{em}= 575 nm for $KCa(PO_3)_3$: x Dy^{3+} (x = 1.0, 2.0, 3.0, 4.0, and 5.0 mol%) ions phosphor are represented in Fig.4.2.7(a). The decaycurves were fitted with various exponential equations; however, for all concentrations of Dy^{3+}ions, the bi-exponential equation showed the best fit. This suggests that dopant ions are interacting significantly, leading to energy transfer from excited Dy^{3+} ions (donor) to unexcited Dy^{3+} ions (acceptor) and that the RE ions in the phosphor lattice are probably going to acquire two different crystallographic sites[30].

The following equation can be used to represent the luminous intensity:

$$I = I_o + A_1 \exp\left(\frac{-t}{\tau_1}\right) + A_2 \exp\left(\frac{-t}{\tau_2}\right) \qquad (8)$$

Where I_O and I represent, respectively, the luminescence intensities at time t = 0 and some other point in time. A_1 and A_2 are the fit constants for bi-exponential fitting, and τ_1 and τ_2 are the components for rapid and slow decay, respectively. When modeling a bi-exponential curve, the average lifetime values are provided by:

$$\tau_{exp} = \frac{A_1(\tau_1)^2 + A_2(\tau_2)^2}{A_1\tau_2 + A_1\tau_2} \qquad (9)$$

The as-synthesized $KCa(PO_3)_3$: xDy^{3+} (x = 1.0, 2.0, , 4.0, and 5.0 mol%) phosphor have τ_{exp} values of 377.74, 327.04, 314.21, 308.84, and 293.03μs, respectively. It was observed that when the quantity of Dy^{3+} ions in the phosphors was increased, the values of τ_{exp} decreased[31].

The decrement in a lifetime values with the increase in the concentration of Dy^{3+} ions was further examined by Auzel's model utilizing equation given below:

$$\tau = \frac{\tau_o}{1+\frac{w}{w_o}e^{-\frac{N}{3}}} \qquad (10)$$

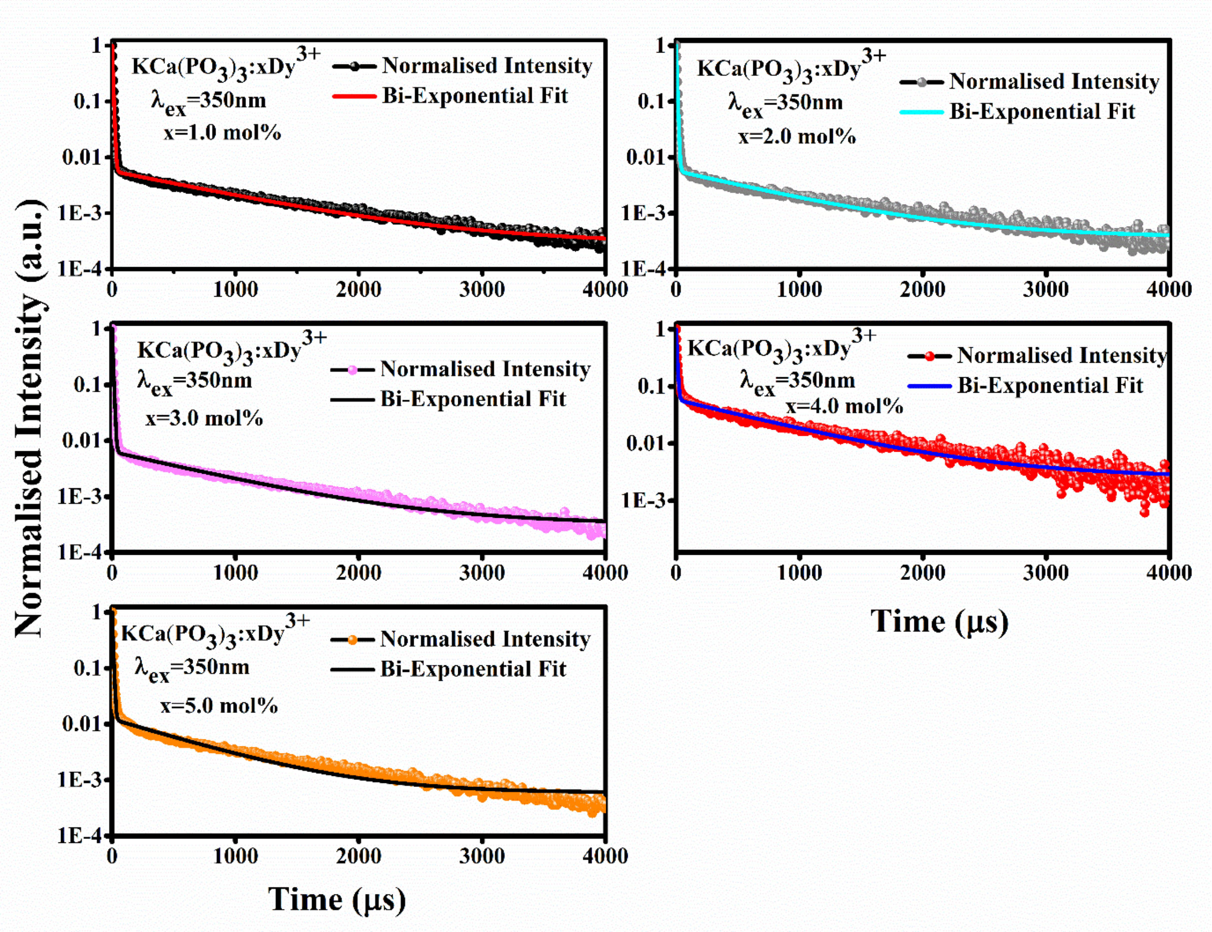

Fig 4.2.7:- PL decay profiles of Dy^{3+} ions doped $KCa(PO_3)_3$ phosphors at λ_{ex} = 350 nm wavelength.

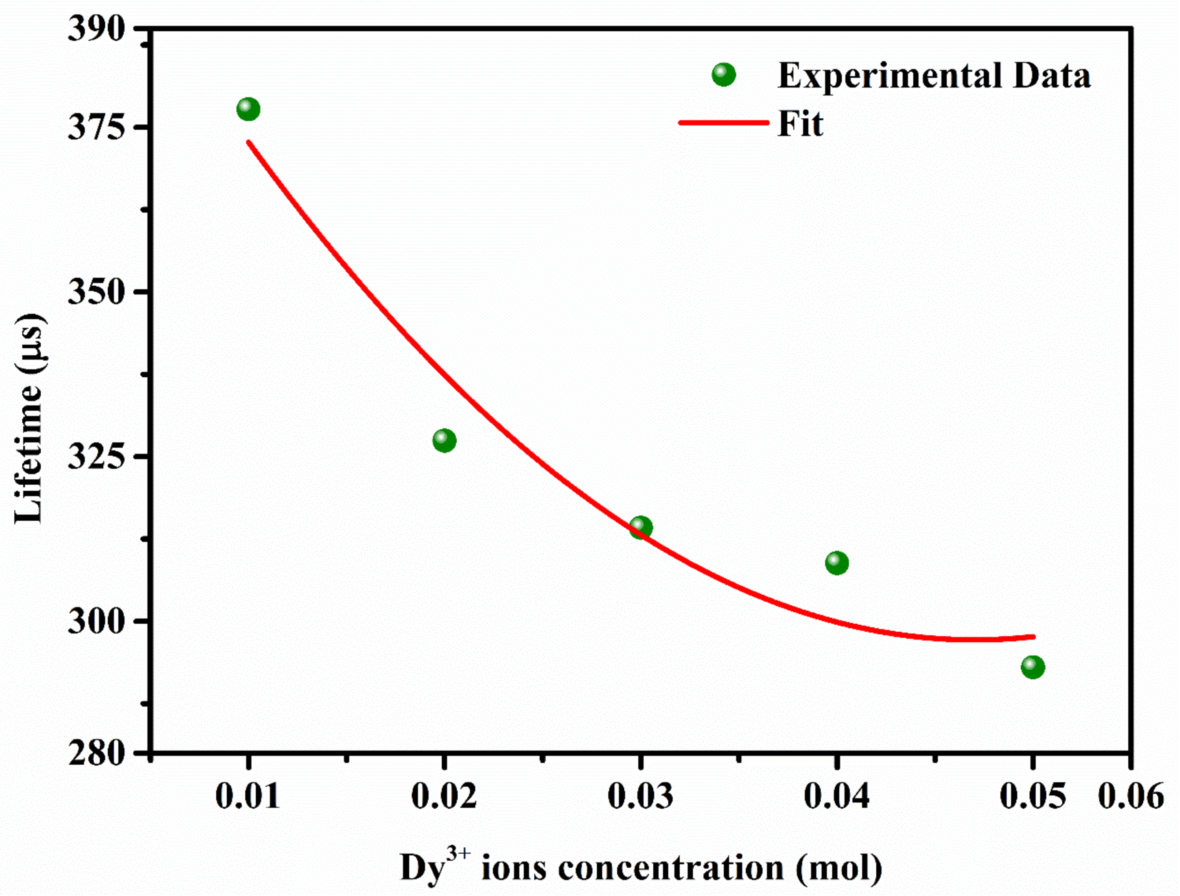

Fig. 4.2.7(b):- Dependence of photoluminescence decay lifetime of the $^4F_{9/2}$ state on the doping. concentration of Dy^{3+} based on Auzel's model.

where τ represents the calculated lifetime, τ_0 represents the intrinsic radiative lifetime, c stands for concentration of Dy^{3+} ions, c_0 represents a constant and N denotes the number of phonons generated during the relaxation. Fig. 13 demonstrates that the Dy^{3+} decay lifetime in KCP phosphor fits well with Auzel's model and the value of τ_0 from the fitting is 419.07 µs.

The quantum efficiency (η) is computed using intrinsic lifetime value as follows.

$$\eta = \frac{\tau}{\tau_o} = \frac{A_R}{A_R + A_{nR}} \qquad (11)$$

Table 4.2.7: Photoluminescence decay lifetime, non-radiative rate and quantum efficiency of

theKCP : xDy^{3+} (x = 1.0, 2.0, , 4.0, and 5.0 mol%) phosphors.

Sample ID KCP: xDy^{3+}	**Decay Lifetime (µs)**	**Non radiative rate (s^{-1})**	**Quantum Efficiency (%)**
x = 1.0mol%	377.74	261.0874	90.13769
x = 2.0mol%	327.04	671.4629	78.04026
x = 3.0mol%	314.21	796.3153	74.97871
x = 4.0mol%	308.84	851.6643	73.69702
x = 5.0mol%	293.03	1026.43	69.92292

$$\frac{1}{\tau} = \frac{1}{\tau_o} + A_{nR} \quad (12)$$

here the rate of relaxation by non-radiative and radiative mechanisms are denoted by A_{nR} and A_R, respectively. Table 2 shows quantum efficiency values (%) along with decay lifetime and non-radiative rates (s^{-1}) for $^4F_{9/2}$ state[32].

CHAPTER 5:- CONCLUSION AND FUTURE SCOPE

5.1 CONCLUSION

In our work, Dy^{3+} doped $KCa(PO_3)_3$ phosphors were successfully synthesized via conventional solid-state reaction technique and were investigated their structural, morphological, and PL characteristics. First, the phase purity of the produced samples was confirmed by analyzing the XRD patterns. $KCa(PO_3)_3$: Dy^{3+} formed a hexagonal structure when it crystallized with a P-6c2(188) space group. Using SEM, morphological analysis was performed, and particle sizes were determined to be in the micrometre (3-5μm) range. Multiple molecular bonds that are present in the structure are shown by the FT-IR spectra. The band gap values, 4.60 & 4.49 eV for undoped and 4.0 mol% of Dy^{3+}, were determined by linear fitting of the tauc plot of Dy^{3+} in the $KCa(PO_3)_3$ host. The excitation spectra show that the previously stated phosphors can be efficiently excited by n-UV light. A number of experiments were used to characterize the samples' luminescence properties. The PL emission spectra findings demonstrated that the samples generated white light with two prominent peaks at 482 nm (blue band) and 575 nm (yellow band) upon excitation by 350 nm UV radiation. The electronic transitions of dysprosium ions at $^4F_{9/2}\rightarrow{}^6H_{15/2}$ and $^4F_{9/2}\rightarrow{}^6H_{13/2}$ were matched by these peaks, respectively. Concentration quenching was observed for Dy^{3+} doping at a concentration of 4.0% mole. The main cause of this quenching was found to be dipole-dipole energy transfer. The computed CIE chromaticity coordinates for $KCa(PO_3)_3$ for 4.0mol% of the Dy^{3+} phosphor lie in the deepwhite area. The PL decay profile displays bi-exponential behavior with decay times being in microseconds (μs) range. As the concentration of Dy^{3+} ions increases, the computed τ_{exp} values decrease because of the transfer of energy between Dy^{3+} - Dy^{3+} ions.The results of the aforementioned studies on the as prepared KCP:Dy^{3+} phosphor highlight that these materials can be used for white light generating LEDs and other photonic devices applications.

5.2 Future Scope

Dysprosium (Dy^{3+}) doping into KCP host material has been the focus of current work, yielding an efficient and superior phosphor that can be employed in inexpensive phosphor-converted white light-emitting diodes (pc-w-LEDs). First, co-doping these phosphors with other appropriate rare-earth ions (RE), including yttrium (Y^{3+}), can improve their luminous qualities. The reason for this is because a new class of quantum integrated photonic devices may be made possible by RE ions co-doped in particular host matrix regions. The current phosphor was created using a traditional solid-state reaction method, and its structural and photoluminescence characteristics have been described. To enhance the particle shape and decrease the particle size, a different synthesis technique like the sol-gel approach can be investigated.

Using nitrates as metal precursors, the solgel combustion method combines the sol-gel and combustion processes. In the Sol–gel method, the metal oxides that are produced undergo a number of reactions. The metal hydroxide solution is condensed to produce gels after the metal nitrate is quickly hydrolyzed, and xerogel is formed during the evaporation process and is subsequently burned at a high temperature. The final product is a fluffy, black structure that is sintered at different temperatures. This technique could be investigated to enhance the phosphor's luminous characteristics in its prepared state. These phosphors' usefulness extends beyond w-LEDs and includes a variety of other applications, including bio-imaging, heat sensors, fingerprint detection, and more.

References:

[1] Y. Li, M. Gecevicius, J. Qiu, Long persistent phosphors - From fundamentals to applications, Chem. Soc. Rev. 45 (2016) 2090–2136. https://doi.org/10.1039/c5cs00582e.

[2] X. Wang, Q. Liu, Y. Bu, C.S. Liu, T. Liu, X. Yan, Optical temperature sensing of rare-earth ion doped phosphors, RSC Adv. 5 (2015) 86219–86236. https://doi.org/10.1039/c5ra16986k.

[3] K. Bando, K. Sakano, Y. Noguchi, Y. Shimizu, Development of High-bright and Pure-white LED Lamps, J. Light Vis. Environ. 22 (1998) 2–5. https://doi.org/10.2150/jlve.22.1_2.

[4] N.C. George, K.A. Denault, R. Seshadri, Phosphors for solid-state white lighting, Annu. Rev. Mater. Res. 43 (2013) 481–501. https://doi.org/10.1146/annurev-matsci-073012-125702.

[5] J. Wang, J. Wang, P. Duan, Luminescent properties of Dy^{3+} doped Sr3Y(PO 4)3 for white LEDs, Mater. Lett. 107 (2013) 96–98. https://doi.org/10.1016/j.matlet.2013.06.001.

[6] N. Narendran, J.D. Bullough, N. Maliyagoda, A. Bierman, What is useful life for white light leds?, J. Illum. Eng. Soc. 30 (2001) 57–67. https://doi.org/10.1080/00994480.2001.10748334.

[7] Y. Ohno, Spectral design considerations for white LED color rendering, Opt. Eng. 44 (2005) 111302. https://doi.org/10.1117/1.2130694.

[8] T. Krishnapriya, A. Jose, T. Anna Jose, C. Joseph, N. V. Unnikrishnan, P.R. Biju, Luminescent kinetics of Dy^{3+} doped $CaZn_2(PO_4)_2$ phosphors for white light emitting applications, Adv. Powder Technol. 32 (2021) 1023–1032. https://doi.org/10.1016/j.apt.2021.02.003.

[9] S. Wang, C. Xu, X. Qiao, Enhanced photoluminescence of red-emitting $KCa(PO_3)_3$: Eu^{3+} phosphors by charge compensation, Opt. Mater. (Amst). 107 (2020) 110102. https://doi.org/10.1016/j.optmat.2020.110102.

[10] D. Zhao, S.R. Zhang, Y.P. Fan, B.Z. Liu, R.J. Zhang, Thermally Stable Phosphor $KBa_2(PO_3)_5$:Eu^{2+} with Broad-Band Cyan Emission Caused by Multisite Occupancy of Eu^{2+}, Inorg. Chem. 59 (2020) 8789–8799. https://doi.org/10.1021/acs.inorgchem.0c00428.

[11] A. Watras, A. Matraszek, P. Godlewska, I. Szczygieł, J. Wojtkiewicz, B. Brzostowski, G. Banach, J. Hanuza, P.J. Dereń, The role of the Ca vacancy in the determination of the europium position in the energy gap, its valence state and spectroscopic properties in $KCa(PO_3)_3$, Phys. Chem. Chem. Phys. 16 (2014) 5581–5588. https://doi.org/10.1039/c3cp54875a.

[12] W. Tang, Q. Guo, K. Su, H. Liu, Y. Zhang, L. Mei, L. Liao, Structure and Photoluminescence Properties of Dy^{3+} Doped Phosphor with Whitlockite Structure, Materials (Basel). 15 (2022) 4–13. https://doi.org/10.3390/ma15062177.

[13] A.K. Bedyal, A.K. Kunti, V. Kumar, H.C. Swart, Effects of cationic substitution on the luminescence behavior of Dy^{3+} doped orthophosphate phosphor, J. Alloys Compd. 806 (2019) 1127–1137. https://doi.org/10.1016/j.jallcom.2019.07.305.

[14] M. Ferhi, S. Toumi, K. Horchani-Naifer, M. Ferid, Single phase $GdPO_4$: Dy^{3+} microspheres blue, yellow and white light emitting phosphor, J. Alloys Compd. 714 (2017) 144–153. https://doi.org/10.1016/j.jallcom.2017.04.193.

[15] C.M. Nandanwar, N.S. Kokode, A.N. Yerpude, S.J. Dhoble, Luminescence properties of $LaPO_4$:RE (RE = Dy^{3+}, Eu^{3+}, Sm^{3+}) orthophosphate phosphor for n-UV solid-state lighting prepared by wet chemical synthesis, J. Mater. Sci. Mater. Electron. 34 (2023) 1–8. https://doi.org/10.1007/s10854-023-10119-0.

[16] K.N. Shinde, S.J. Dhoble, A. Kumar, Synthesis of novel Dy^{3+} activated phosphate phosphors for NUV excited LED, J. Lumin. 131 (2011) 931–937. https://doi.org/10.1016/j.jlumin.2010.12.026.

[17] S. Kumari, A.S. Rao, R.K. Sinha, Structural and photoluminescence properties of Sm^{3+} ions doped strontium yttrium tungstate phosphors for reddish-orange photonic device applications, Mater. Res. Bull. 167 (2023). https://doi.org/10.1016/j.materresbull.2023.112419.

[18] K. Munirathnam, G.R. Dillip, S. Chaurasia, S.W. Joo, B. Deva Prasad Raju, N. John Sushma, Investigations on surface chemical analysis using X-ray photoelectron spectroscopy and optical properties of Dy^{3+}-doped $LiNa_3P_2O_7$ phosphor, J. Mol. Struct. 1118 (2016) 117–123. https://doi.org/10.1016/j.molstruc.2016.04.004.

[19] R. Mahajan, S. Kumar, R. Prakash, V. Kumar, R.J. Choudhary, D.M. Phase, X-ray photoemission and spectral investigations of Dy^{3+} activated magnesium pyrophosphate phosphors, J. Alloys Compd. 777 (2019) 562–571. https://doi.org/10.1016/j.jallcom.2018.10.355.

[20] V. Vidyadharan, E. Sreeja, S.K. Jose, C. Joseph, N. V. Unnikrishnan, P.R. Biju, Spectroscopic and photoluminescence characterization of Dy^{3+} in $Sr_{0.5}Ca_{0.5}TiO_3$ phosphor, Luminescence 31 (2016) 202–209. https://doi.org/10.1002/bio.2946.

[21] Y. Wang, X. Liu, L. Jing, P. Niu, Tunable white light and energy transfer of Dy^{3+} and Eu^{3+} doped $Y_2Mo_4O_{15}$ phosphors, Ceram. Int. 42 (2016) 13004–13010. https://doi.org/10.1016/j.ceramint.2016.05.075.

[22] U. Fawad, H.J. Kim, S. Khan, M. Khan, L. Ali, Photoluminescent properties of white-light-emitting $Li_6Y(BO_3)_3:Dy^{3+}$ phosphor, Solid State Sci. 62 (2016) 1–5. https://doi.org/10.1016/j.solidstatesciences.2016.08.008.

[23] R. Faoro, F. Moglia, M. Tonelli, N. Magnani, E. Cavalli, Energy levels and emission parameters of the Dy^{3+} ion doped into the YPO_4 host lattice, J. Phys. Condens. Matter 21 (2009). https://doi.org/10.1088/0953-8984/21/27/275501.

[24] W.T. Carnall, P.R. Fields, K. Rajnak, Electronic energy levels of the trivalent lanthanide aquo ions. IV. Eu^{8+}, J. Chem. Phys. 49 (1968) 4424–4442. https://doi.org/10.1063/1.1669893.

[25] T. Wang, Y. Hu, L. Chen, X. Wang, M. He, An intense single-component warm-white-light $Sr_3Lu(PO_4)_3:Dy^{3+}$ phosphor for white UV-LEDs, J. Mater. Sci. Mater. Electron. 27 (2016) 13235–13241. https://doi.org/10.1007/s10854-016-5470-9.

[26] R. Vijayakumar, G. Venkataiah, K. Marimuthu, Structural and luminescence studies on Dy3+ doped boro-phosphate glasses for white LED’s and laser applications, J. Alloys Compd. 652 (2015) 234–243. https://doi.org/10.1016/j.jallcom.2015.08.219.

[27] W. Huang, Q. Liu, X. Li, Q. Zhu, L. Wang, Q. Zhang, Dy^{3+}-doped $BaLaMgSbO_6$ double perovskite highly efficient white phosphor, Ceram. Int. 45 (2019) 15624–15628. https://doi.org/10.1016/j.ceramint.2019.05.073.

[28] Q. Su, H. Liang, C. Li, H. He, Y. Lu, J. Li, Y. Tao, Luminescent materials and spectroscopic properties of Dy^{3+} ion, J. Lumin. 122–123 (2007) 927–930. https://doi.org/10.1016/j.jlumin.2006.01.329.

[29] T. Verma, S. Agrawal, Optical studies and estimation of kinetic parameters for dysprosium activated yttrium oxide phosphors, Optik (Stuttg). 160 (2018) 361–370. https://doi.org/10.1016/j.ijleo.2018.02.015.

[30] S. Dutta, S. Som, S.K. Sharma, Excitation spectra and luminescence decay analysis of K^+ compensated Dy^{3+} doped $CaMoO_4$ phosphors, RSC Adv. 5 (2015) 7380–7387. https://doi.org/10.1039/c4ra12447b.

[31] P. Kumari, J. Manam, Structural, optical and special spectral changes of Dy^{3+} emissions in orthovanadates, RSC Adv. 5 (2015) 107575–107584. https://doi.org/10.1039/c5ra18982a.

[32] J. Sun, X. Zhang, Z. Xia, H. Du, Synthesis and luminescence properties of novel $LiSrPO_4:Dy^{3+}$ phosphor, Mater. Res. Bull. 46 (2011) 2179–2182. https://doi.org/10.1016/j.materresbull.2011.07.033.

Plagiarism Report

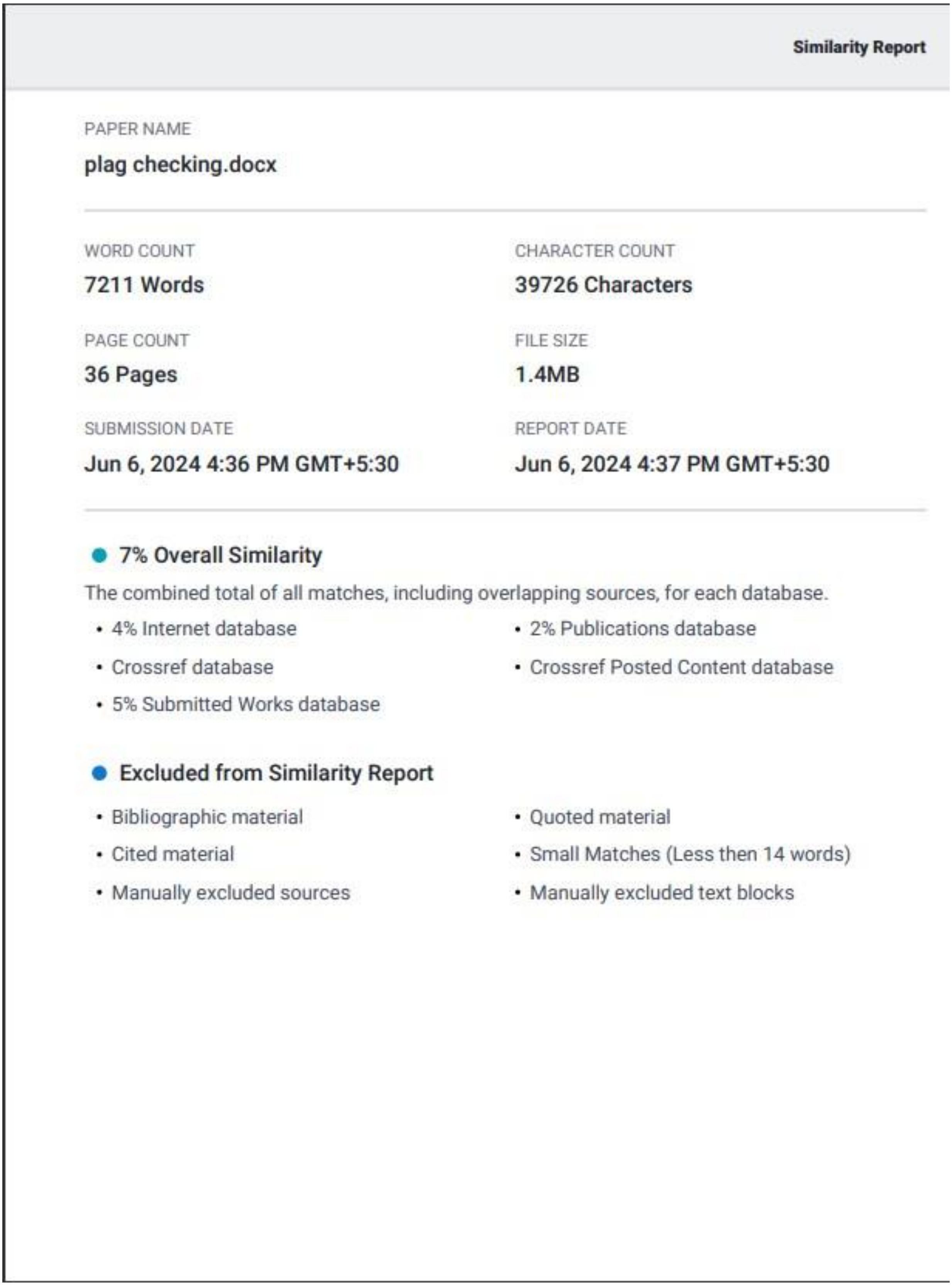

Similarity Report

PAPER NAME

plag checking.docx

WORD COUNT **7211 Words**	CHARACTER COUNT **39726 Characters**
PAGE COUNT **36 Pages**	FILE SIZE **1.4MB**
SUBMISSION DATE **Jun 6, 2024 4:36 PM GMT+5:30**	REPORT DATE **Jun 6, 2024 4:37 PM GMT+5:30**

● 7% Overall Similarity

The combined total of all matches, including overlapping sources, for each database.

- 4% Internet database
- 2% Publications database
- Crossref database
- Crossref Posted Content database
- 5% Submitted Works database

● Excluded from Similarity Report

- Bibliographic material
- Quoted material
- Cited material
- Small Matches (Less then 14 words)
- Manually excluded sources
- Manually excluded text blocks

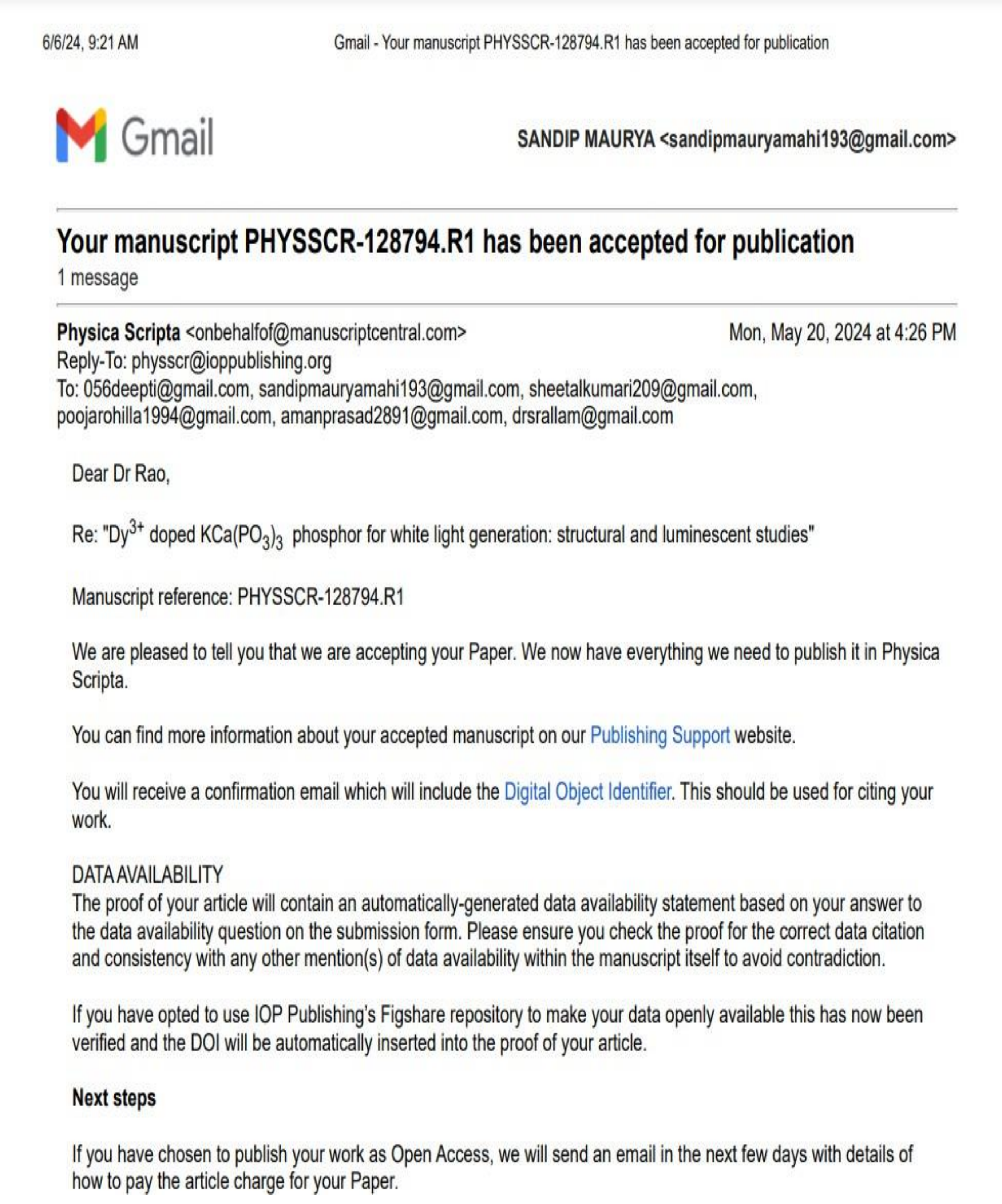

6/6/24, 9:21 AM Gmail - Your manuscript PHYSSCR-128794.R1 has been accepted for publication

Gmail **SANDIP MAURYA <sandipmauryamahi193@gmail.com>**

Your manuscript PHYSSCR-128794.R1 has been accepted for publication

1 message

Physica Scripta <onbehalfof@manuscriptcentral.com> Mon, May 20, 2024 at 4:26 PM
Reply-To: physscr@ioppublishing.org
To: 056deepti@gmail.com, sandipmauryamahi193@gmail.com, sheetalkumari209@gmail.com, poojarohilla1994@gmail.com, amanprasad2891@gmail.com, drsrallam@gmail.com

Dear Dr Rao,

Re: "Dy^{3+} doped $KCa(PO_3)_3$ phosphor for white light generation: structural and luminescent studies"

Manuscript reference: PHYSSCR-128794.R1

We are pleased to tell you that we are accepting your Paper. We now have everything we need to publish it in Physica Scripta.

You can find more information about your accepted manuscript on our Publishing Support website.

You will receive a confirmation email which will include the Digital Object Identifier. This should be used for citing your work.

DATA AVAILABILITY
The proof of your article will contain an automatically-generated data availability statement based on your answer to the data availability question on the submission form. Please ensure you check the proof for the correct data citation and consistency with any other mention(s) of data availability within the manuscript itself to avoid contradiction.

If you have opted to use IOP Publishing's Figshare repository to make your data openly available this has now been verified and the DOI will be automatically inserted into the proof of your article.

Next steps

If you have chosen to publish your work as Open Access, we will send an email in the next few days with details of how to pay the article charge for your Paper.

DEPARTMENT OF APPLIED PHYSICS

DELHI TECHNOLOGICAL UNIVERSITY

(Formerly Delhi College of Engineering)

PUBLISHED PAPER PROOF

IOP Publishing Phys. Scr. 99 (2024) 065573 https://doi.org/10.1088/1402-4896/ad4[illegible]

Physica Scripta

RECEIVED
29 February 2024

REVISED
26 April 2024

ACCEPTED FOR PUBLICATION
20 May 2024

PUBLISHED
30 May 2024

PAPER

Dy^{3+} doped $KCa(PO_3)_3$ phosphor for white light generation: structural and luminescent studies

Deepti[1], **Sandip Maurya**[1], **Sheetal Kumari**[1], **Pooja Rohilla**[1], **Aman Prasad**[2] and **A S Rao**[1,*]

[1] Department of Applied Physics, Delhi Technological University, Bawana Road, Delhi, 110042, India

[2] Department of Physics and Computer Science, Dayalbagh Educational Institute (DEI), Deemed University, Dayalbagh, Agra, 282005, India

[*] Author to whom any correspondence should be addressed.

E-mail: drsrallam@gmail.com

Keywords: XRD, phosphor, photoluminescence, CIE coordinates

Abstract

Using the traditional solid-state reaction approach, Dy^{3+} ions doped $KCa(PO_3)_3$ phosphors have been synthesized to investigate their luminescent properties to produce high-quality white light for solid-state lighting applications, particularly in white LEDs. x-ray diffraction (XRD) patterns were used to examine the structure and phase of the phosphors. Using scanning electron microscopy (SEM), the morphology of the as-synthesized phosphor has been investigated. Fourier transform infrared spectroscopy (FT-IR) has been used to investigate several vibrational bands seen in the phosphor. Using diffuse reflectance spectra (DRS), the as-synthesized phosphors' optical band gap values have been estimated. When Dy^{3+} ions are excited at 350 nm, the photoluminescence (PL) spectra characteristics observed for the activated $KCa(PO_3)_3$ phosphor show strong white area emission due to both 575 nm, which is related to the $^4F_{9/2} \rightarrow {}^6H_{13/2}$ and 482 nm that is ascribed to $^4F_{9/2} \rightarrow {}^6H_{15/2}$ transition of Dy^{3+} ions. Additionally, the concentration quenching of Dy^{3+} ions doped at 4 mol% is seen in the PL spectra. Based on the observed PL spectra, the computed CIE chromaticity coordinates for the optimised $KCa(PO_3)_3$ phosphors are located in the deep white area. The lifespan of the as-titled phosphors decreases as the amount of Dy^{3+} ions increases in the host lattice. Additionally, the PL decay profiles shows a dual exponential behaviour when excited at 350 nm, with an emission wavelength at 575 nm. The lifetime values were used to calculate the quantum efficiency of the as prepared phosphors. On the basis of the results of the aforementioned studies, we wish to project Dy^{3+} ion doped $KCa(PO_3)_3$ phosphors as white light generating materials in w-LEDs and for other photonic applications.

1. Introduction

Phosphors are widely used in solid-state lighting, display devices, and anti-counterfeiting applications [1, 2]. White light-emitting diodes (w- LEDs) have gained popularity in recent years due to their low power consumption and environmental benefits. They are expected to replace traditional light sources such as tungsten halogen lamps and incandescent lamps. LEDs have a significantly longer lifespan when compared to other lighting technologies like Low-Pressure Sodium (LPS) and fluorescent lights. The longevity of LEDs far surpasses that of incandescent lights. The latest LED lights can last for over 50,000 to 100,000 h or more. In contrast, incandescent bulbs have a lifespan that is only 1%–5% as long at best, lasting for approximately 1,200 h. The additional features of these properties include a broad spectrum of colors that span from ultraviolet to infrared, a limited spectral bandwidth, a high degree of luminous efficiency, and an extremely rapid response time [3, 4]. The most common method for creating white LEDs is to combine phosphors with UV or n-UV chips made of InGaN. The development process of the standard LED involves three crucial steps: seasoning, selection, and certification. These steps are meticulously carried out to ensure the optimal performance of the w-LED [5–7]. During seasoning, the LED is subjected to a series of tests to stabilize its electrical and thermal properties. The

CONFERENCE ACCEPTED PROOF

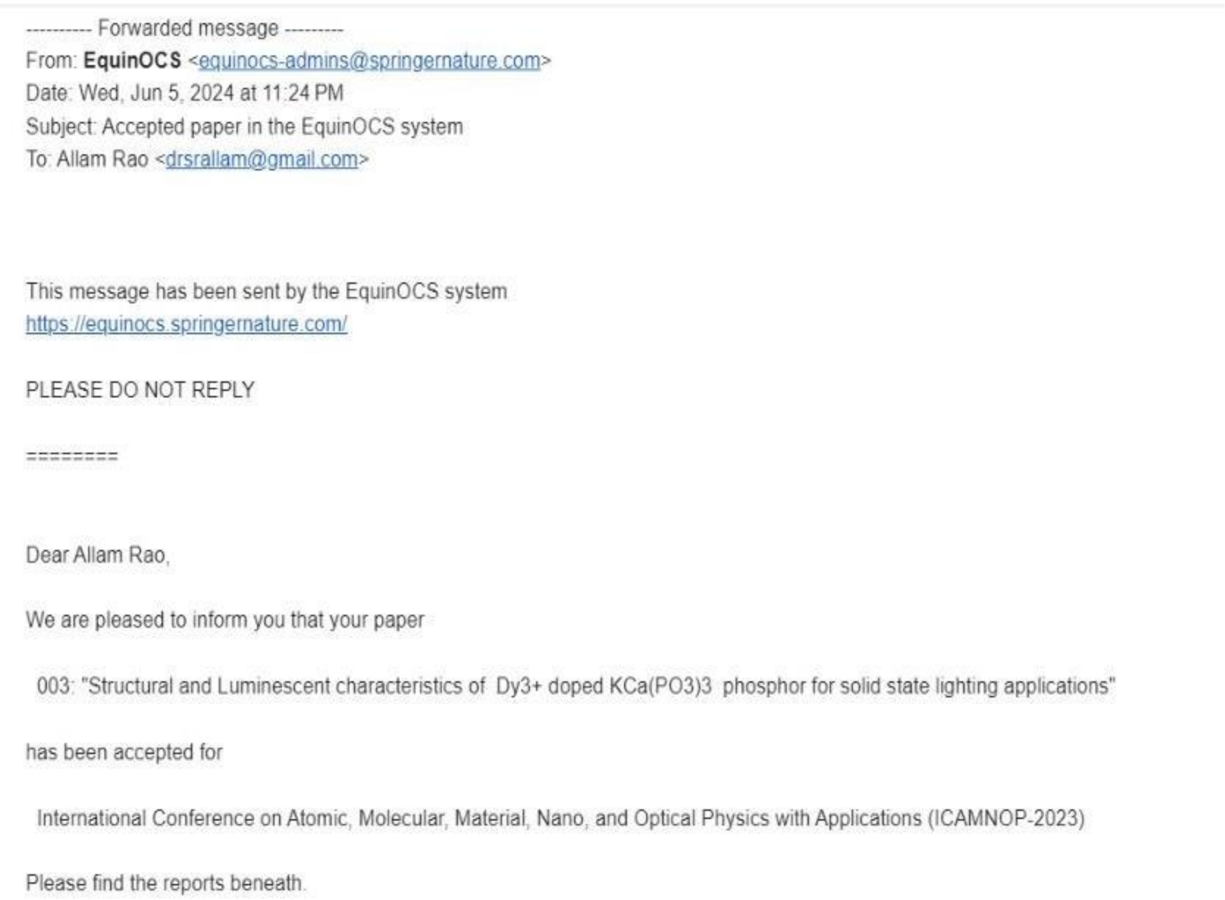

---------- Forwarded message ---------

From: **EquinOCS** <equinocs-admins@springernature.com>

Date: Wed, Jun 5, 2024 at 11:24 PM

Subject: Accepted paper in the EquinOCS system

To: Allam Rao <drsrallam@gmail.com>

This message has been sent by the EquinOCS system

https://equinocs.springernature.com/

PLEASE DO NOT REPLY

========

Dear Allam Rao,

We are pleased to inform you that your paper

003: "Structural and Luminescent characteristics of Dy3+ doped KCa(PO3)3 phosphor for solid state lighting applications"

has been accepted for

International Conference on Atomic, Molecular, Material, Nano, and Optical Physics with Applications (ICAMNOP-2023)

Please find the reports beneath.

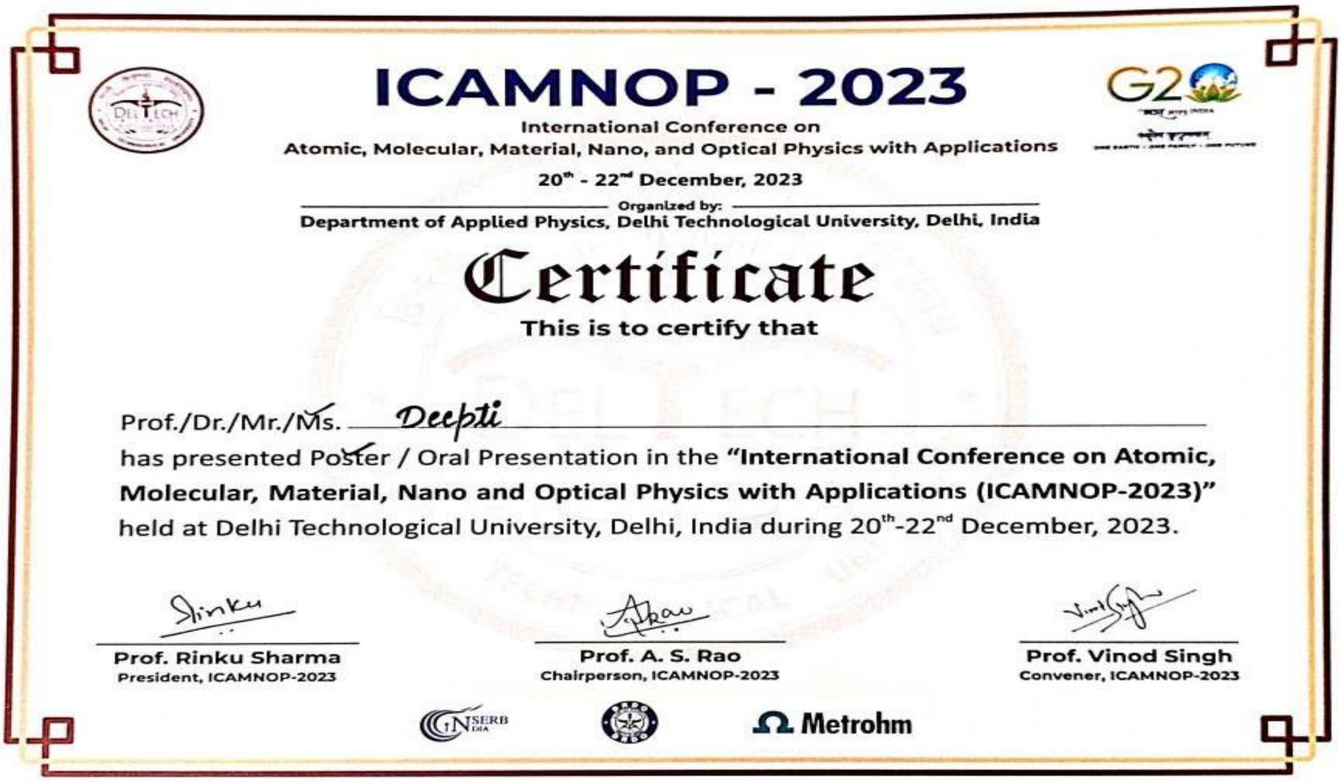

ICAMNOP - 2023

International Conference on
Atomic, Molecular, Material, Nano, and Optical Physics with Applications
20th - 22nd December, 2023

Organized by:
Department of Applied Physics, Delhi Technological University, Delhi, India

Certificate

This is to certify that

Prof./Dr./Mr./[✓ Ms.] Deepti
has presented [✓ Poster] / Oral Presentation in the **"International Conference on Atomic, Molecular, Material, Nano and Optical Physics with Applications (ICAMNOP-2023)"** held at Delhi Technological University, Delhi, India during 20th-22nd December, 2023.

Rinku
Prof. Rinku Sharma
President, ICAMNOP-2023

ASRao
Prof. A. S. Rao
Chairperson, ICAMNOP-2023

Vinod Singh
Prof. Vinod Singh
Convener, ICAMNOP-2023

ICAMNOP - 2023

International Conference on
Atomic, Molecular, Material, Nano, and Optical Physics with Applications
20th - 22nd December, 2023

Organized by:
Department of Applied Physics, Delhi Technological University, Delhi, India

Certificate

This is to certify that

Prof./Dr./[✓ Mr.]/Ms. Sandip Maurya
has presented [✓ Poster] / Oral Presentation in the **"International Conference on Atomic, Molecular, Material, Nano and Optical Physics with Applications (ICAMNOP-2023)"** held at Delhi Technological University, Delhi, India during 20th-22nd December, 2023.

Rinku
Prof. Rinku Sharma
President, ICAMNOP-2023

ASRao
Prof. A. S. Rao
Chairperson, ICAMNOP-2023

Vinod Singh
Prof. Vinod Singh
Convener, ICAMNOP-2023

Scopus indexing profile

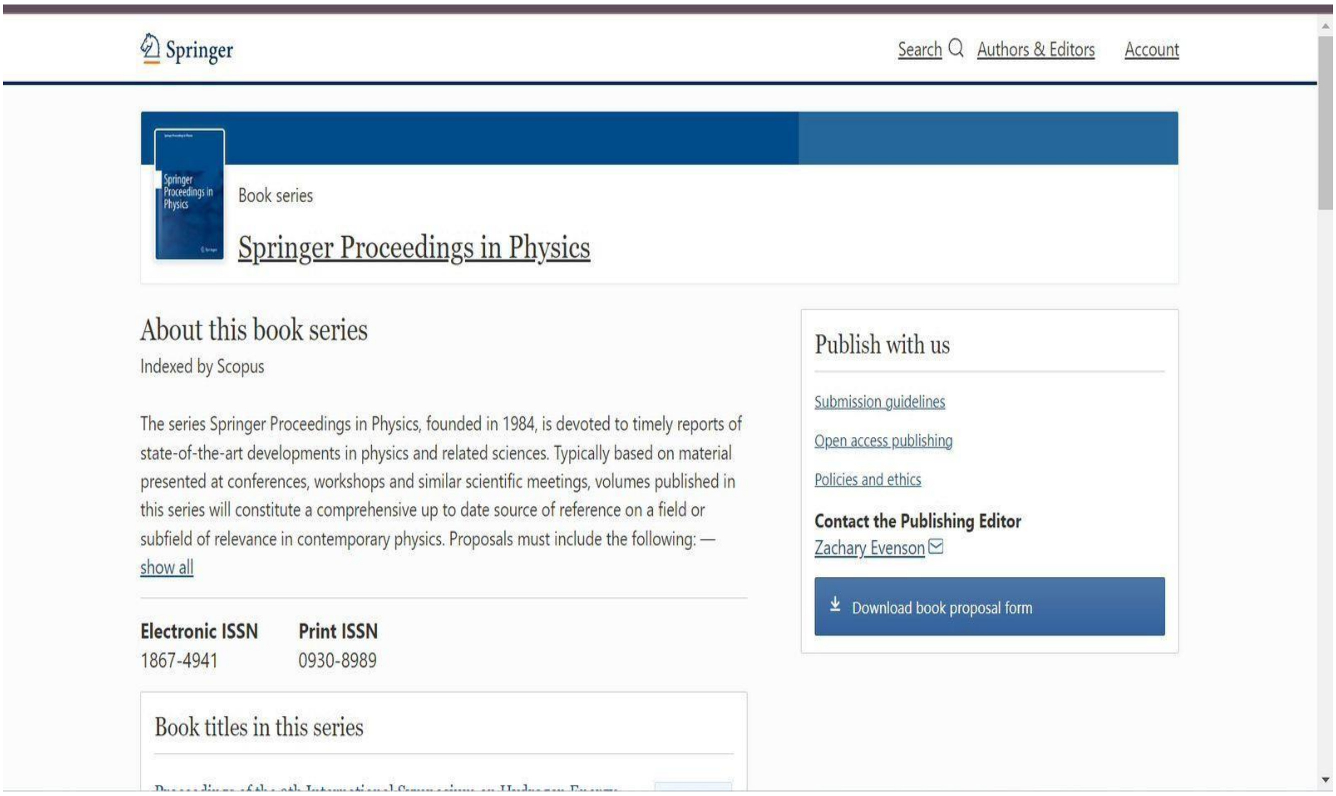

Book series

Springer Proceedings in Physics

About this book series

Indexed by Scopus

The series Springer Proceedings in Physics, founded in 1984, is devoted to timely reports of state-of-the-art developments in physics and related sciences. Typically based on material presented at conferences, workshops and similar scientific meetings, volumes published in this series will constitute a comprehensive up to date source of reference on a field or subfield of relevance in contemporary physics. Proposals must include the following: — show all

Electronic ISSN 1867-4941

Print ISSN 0930-8989

Book titles in this series

Publish with us

Contact the Publishing Editor
Zachary Evenson


International Conference on Atomic, Molecular, Material, Nano and Optical Physics with Applications (ICAMNOP–2023)

Organized by: Department of Applied Physics, Delhi Technological University Delhi-110042, India

December 20th-22nd, 2023

About The Conference

The International Conference on Atomic, Molecular, Material, Nano and Optical Physics with Applications (ICAMNOP 2023) will focus on developments in atomic, molecular, material, Nano and Optical Physics which have proved to be powerful science supporting many other areas of science & technology, including industrial, information, energy, global Change, defense, health and medical environmental, space and transportation technology. The conference will involve experimental and theoretical studies of atoms, ions, molecules and nanostructures both at the fundamental level & on the application side using advanced technology. Using modern tools of high – field and ultra-fast physics, one no longer merely observes nature, but can reshape and redirect atoms, molecules, particles or radiation. This new drive towards harnessing quantum dynamics is enormously important to future developments in fundamentals physics and applied energy science. Third generation synchrotron sources offer new opportunities to study radiation – matter interactions. Optical techniques have also played a very important role in the creation, understanding and manipulation of atomic and molecular Bose- Einstein Condensates. Complete quantum mechanical description of such properties and interactions is required and to this end, the present conference aims at bringing together experimental and theoretical scientists working in various fields of "Atomic, Molecular, Material, Nano and Optical Physics", to share and exchange new ideas. Topics of interest in the conference include: Atomic & Molecular Structure, Collision Process, clusters, surfaces and exotic particles and Applications, Laser cooling, trapping and Bose – Einstein condensation, High precision and Ultracold phenomena, High harmonic generation and applications, Coherent optical phenomena, Ultrafast dynamics at the Femto- or Atto second scale, ion – include radiation damage in particular of biomolecules, atomic spectroscopy and molecular physics of antimatter, free electron laser, particle acceleration generated by high – power laser, Quantum optics and its application to Mesoscopic system, Other topics covered are: Spectroscopy of Solar and Stellar Plasma, The atomic universe: Spectra as Probes of Cool Gas. The rapidly growing field of nanophysics is introduced as a separate conference topic this time, which include, Nano-structures and Photonics. In the last, a session will also be devoted to application of Atomic, Molecular Optical and Nano Physics in Petroleum, Renewable energy, Environmental Science, Information Technology, Health and Education in Developing Countries.